Implementation of lookup tables for different optimization strategies of semi-active car suspension system

Aurimas Čerškus[1], Nikolaj Šešok[2], Vytautas Bučinskas[3]
Department of Mechatronics, Robotics and Digital Manufacturing, Vilnius Gediminas Technical University, Vilnius, Lithuania
[3]Corresponding author
E-mail: [1]*aurimas.cerskus@vilniustech.lt*, [2]*nikolaj.sesok@vilniustech.lt*, [3]*vytautas.bucinskas@vilniustech.lt*

Received 26 November 2024; accepted 4 February 2025; published online 5 April 2025
DOI https://doi.org/10.21595/jve.2025.24689

Abstract. Road irregularities and various vehicle loads influence comfort and safety levels. Owing to these changes, the driver cannot quickly and easily find the best driving parameters. Control of damping in a semi-active suspension adjusts the damping process in the vehicle to minimize the acceleration of the crew. This ensures comfort for them, influencing the level of fatigue of the driver and safe driving. A theoretical analysis was implemented using a mathematical full-car model in Simulink/MATLAB. We performed a simulation of a vehicle with all passengers passing various artificially generated road profiles at different velocities. We optimized the damping coefficient for the maximum comfort level using one, two, or four damping values, implementing different optimization strategies. The obtained research results were finalized by the conclusions.

Keywords: semi-active suspension, vehicle damping, optimization, ride comfort, optimization strategy.

1. Introduction

One of the key systems in a vehicle is the suspension, which helps to maintain uninterrupted and good touch of the tires with the road and assures driving safety and ride comfort irrespective of the quality of the road surface or weather conditions [1]-[3]. The suspension can be passive, fully active, or semi-active. Typically, passive suspension systems have limited isolation or motion control. The crew is best isolated from low-frequency vibrations when damping is high. However, high damping reduces high-frequency absorption. Conversely, when the damping is low, the damper offers sufficient high-frequency absorption and poor low-frequency isolation. D. Karnopp [4] stated that for ride comfort, the suspension should isolate the body from high-frequency road inputs. However, at lower frequencies, the body and wheel should closely follow the vertical input from the road. This is related to vehicle handling. Thus, the increased damping in the suspension system deteriorates comfort but improves safety. The intuitive relationship between comfort and safety is discrepant [1], [5], [6], and it is not viable to improve both at the same time. Meanwhile, the authors [7], [8] showed that the dependence of modified comfort and safety indicators on some damping ranges of damping increases and decreases consistently. Another possible solution to this compromise is the semi-active hydropneumatic spring-damper system proposed by P.S. Els et al. [1], in the form of a four-state system, or an active suspension system, or improving driver comfort by optimizing the seat [9]. Various systems have been discussed in references [3], [5], [10]-[12], and their strengths, weaknesses, relative performance, and equipment requirements have been identified. Active suspension systems can improve the performance of suspension systems at wide frequencies compared to passive suspension systems [13]. A semi-active suspension system combines the advantages of other types of suspensions. It can smoothly change damping, be effective nearly as effective as a fully active suspension [14], and is preferred due to its inherent characteristics such as low energy

consumption, especially in vehicles where available power is limited. Semi-active suspensions have attracted considerable attention because their controllable parameters can be adjusted in real-time [15], [16].

One of the steps in designing a suspension system is the evaluation of the dynamic vehicle model. Well-known quarter-car models [10], [17], [18], which exhibit two degrees of freedom (two DOFs), are used to evaluate the decoupling vibrations that occur for an entire vehicle. However, the main disadvantage of quarter-car models is the omission of vibration propagation between all vehicle quarter parts and the fact that the wheelbase filtering effect cannot be captured and would overestimate the bounce acceleration responses of the sprung mass. Some applications require the use of half-car (four DOFs) models [19], [20]. These models can be justified in the case of the symmetrical construction of a vehicle or symmetrical road-induced kinematic excitation. Although it simplifies the analysis of the vehicle dynamics, the half-car model describes only the pitch or roll dynamics of the vehicle. Full-car models [21], [22] with seven DOFs describe a three-dimensional frame with four wheels. In the full-car model, the vertical dynamics of the four wheels as well as the heave, pitch, and roll dynamics of the vehicle body are mapped. Unlike a quarter-car model, a full-car model is a complex model that can register a detailed vehicle's dynamics of vertical motion. Full-car models with a higher number of DOFs are used not only to evaluate more complex vehicle dynamics [24], but also to evaluate the impact of vibrations on the driver or passengers [24]-[32]. The authors considered only the driver, all passengers, or different seating combinations using models of different complexities. However, the masses applied to the entire crew were the same in all the cases.

The other steps are to choose the type, structure, and control of the suspension, metrics of safety or comfort of the ride, and the objective function for optimization. The different emphasis is on ride comfort and handling stability under different road conditions and driving styles. The characteristics of suspensions also need to change according to the driving style and road conditions during driving [1], [33]-[35]. When ride comfort is a priority, a semi-active suspension system with a variable damper can be effective, similar to an active system [11], [12], [17], [36]. Notwithstanding, the variable damper in a semi-active suspension system has significant restrictions when it is necessary to control the height and posture movement of the vehicle. This problem can be solved by using variable stiffness in a semi-active suspension system [37]-[39]. Thus, some authors have applied variable dampers and variable stiffness [40]-[44]. Therefore, semi-active systems are very helpful in improving ride quality and vehicle-handling capacities. Many different control strategies [45]-[50] have been developed to identify control signals by measuring various parameters. These can be based on linear or non-linear models [51]-[54]. The classical strategies for semi-active vibration control are sky-hooks or ground-hooks. Modern and intelligent controllers can use optimal control [55], [56], model predictive control [57], fuzzy-logic control [18], [58], or based on road statistical properties, that is, optimal damping ratio control [59]. Furthermore, the behavior of semi-active systems was improved by implementing a preview strategy [60], [61]. Consequently, information is needed on road conditions.

Researchers have conducted numerous investigations on models or methods of road recognition. Various methods and equipment required for the measurement of road properties were reviewed in [62]-[64]. Meanwhile, not expensive response-based road profile identification methods were reviewed in [65]. Other possibilities could be advances in semi-active suspension design, such as vehicle-to-vehicle or vehicle-to-infrastructure communication, vehicle localization with real-time access to cloud information.

The procedures for the objective evaluation of ride quality are defined in the standard ISO 2631-1:1997 [66]. G. Guastadisegni et al. [67] listed and discussed available metrics for the objective evaluation of vehicle ride quality, and reviewed how available studies have associated metrics with road profiles and manoeuvres. There is a primary difference between the indicators for evaluating ride comfort and those for road holding. When assessing ride comfort, the selection of metrics is affected by the properties of the road profile. Ride comfort metrics are mainly based on the vertical accelerations recorded over time in different positions of the vehicle, and its root

mean square (RMS) value is also the main indicator for long-type road profiles. When evaluating the quality of driving, especially for high-performance passenger cars, it is also necessary to consider the indicators of road holding capability. Thus, can be chosen not only as one indicator but also as a combination of them [68]. Similar to the modified objective function introduced by Z. Lozia [7], [69], it has weighting factors within the range of [0, 1] for comfort and safety indicators. In line with common practice, three criteria can be adopted to assess the correctness of the selection of the suspension damping coefficient: 1) minimization of the measure of vehicle occupants' discomfort, 2) minimization of the safety hazard, and 3) limitation of the working displacements of the suspension system. S. A. Abu Bakar et al. [70] stated that the selected damping value should provide the maximum overall percentage of performance improvement.

We are continuing to research and develop the control of our semi-active suspension system [71] using information obtained from a segment of the driven road profile [72], [73]. The vehicle control block will receive the road characteristics and information about the vehicle load and will set the damper damping values to minimize the vibration of the vehicle body and crew. For this purpose, we need a gridded matrix of the required optimal damping values related to the characteristics of the road at certain fixed values of speed and masses of the crew. In one of our previous papers [74], we showed that only a few points needed for the entire matrix can be found in the literature and presented the results of damping optimization for a driver with various mass locations.

This study provides a relationship between the optimized damping values for a full-car model with 12 DOFs and the detected road characteristics (waviness values w_1, w_2) for a wide range of road profiles travelling through them at various speeds. Here, to minimize the number of possible choice, we focus on the case in which the damping coefficient is optimized for the maximum level of comfort with different fixed crew mass. In addition, the same value of damping, two different or different damping values for all wheels, is used and optimized for the driver, for the driver and front passenger, for the driver and rear left passenger, and for the entire crew.

2. Methods

2.1. Road profiles

Real experiments require the measurement of the road profile. Different direct, non-contact measurements or system response-based estimations can be used. For simulation, it was possible to use a measured real road profile or a generated artificial profile with the prescribed parameters. An artificial random road profile can be generated through the implementation of 1) linear filtering, 2) superposition of harmonics (sinusoidal approximation), and 3) inverse fast Fourier transform of discretized power spectral density (PSD) [75]. We also used one of the most commonly implemented methods [76]-[78] for superposition of harmonics. Longitudinal road profiles were generated using the original MATLAB™ code, implementing the method of superposition of harmonics in the spatial domain according to Eqs. (1-2):

$$z(x) = \sum_{i=1}^{N=(\Omega_U-\Omega_L)/\Delta\Omega} Z_i \cos(\Omega_i x + \varphi_i), \tag{1}$$

$$Z_i = \sqrt{2G_d(\Omega_i)\Delta\Omega}, \tag{2}$$

where Z_i, $\Omega_i = \Omega_L + (i-1)\Delta\Omega$, φ_i are respectively amplitude, angular spatial frequency and uniformly distributed phase angle of ith harmonic; Ω_U, Ω_L, $\Delta\Omega$ are respectively upper or lower angular spatial frequencies in the PSD spectrum and the width of each frequency band; $G_d(\Omega_i)$ is displacement PSD at the angular spatial frequency Ω_i; N is number of harmonics (we used 1000). The ISO 8608 standard recommends the lower and upper limits of the angular spatial frequencies (= $2\pi n$) equal to $2\pi\times0.01$ rad/m and $2\pi\times10$ rad/m for general on-road measurements, respectively

[79]. In order to generate different road profiles that match the real roads more closely, we replaced the linear fitting of $G_d(\Omega)$ proposed by ISO [79] to two split fittings offered by P. Andrén [80] in Eq. (2) and modified it by reducing the amplitude of frequencies higher than Ω_2 and lower than $0.04\times2\pi$ rad/m:

$$G_d(\Omega) = \begin{cases} G_d(\Omega_0)\Omega^{-1}, & \Omega \le 0.04 \times 2\pi \text{ rad/m}, \\ G_d(\Omega_0)\Omega^{-w_1}, & 0.04 \times 2\pi \text{ rad/m} \le \Omega \le \Omega_2, \\ G_d(\Omega_0)\Omega^{-w_2}, & \Omega_1 \le \Omega \le \Omega_2, \\ G_d(\Omega_0)\Omega^{-w_3=5}, & \Omega_2 \le \Omega, \end{cases} \tag{3}$$

where w_i is waviness; $\Omega_0 = 1$ rad/m, $\Omega_1 = 0.21\times2\pi$ rad/m and $\Omega_2 = 1.22\times2\pi$ rad/m. These values of reference, lower, and higher break frequencies, respectively, produced a minimal error for the Swedish road network [80]. In addition, Welch-type window functions have been used to minimize the appearance of sudden shifts in connections between profile segments, with 10 exponential values [81]. The left-hand wheels passed the profile generated in this way, while for the right-hand wheels it was modified by randomly increasing or decreasing it values up to 20 %. An identical random number sequence was used to generate each profile for comparison.

2.2. Dynamic model

The dynamic response of Range Rover Evoque to road irregularities was analyzed using a full-car model with 12 DOFs [82]: seven DOFs for the vehicle body [21] and five DOFs for vertical displacements along the Z-axis of the crew and baggage box masses. In other words, our model included 10 masses (car body, four wheels, driver, three passengers, and baggage box) and two moments of inertia about the X and Y axes and was constructed using Lagrange's equation of the second type in generalized coordinates. These equations were solved analytically, and after differentiation the final system was obtained, which consists of 12 equations presented in this way:

$$\begin{aligned} &a_{ii}\ddot{q}_i + b_{i1}\dot{q}_1 + b_{i2}\dot{q}_2 + \cdots + b_{in}\dot{q}_n + c_{i1}q_1 + c_{i2}q_2 + \cdots + c_{in}q_n \\ &\quad = d_{i1}\eta_1 + d_{i2}\eta_2 + d_{i3}\eta_3 + d_{i4}\eta_4 + d^*_{i1}\dot{\eta}_1 + d^*_{i2}\dot{\eta}_2 + d^*_{i3}\dot{\eta}_3 + d^*_{i4}\dot{\eta}_4, \end{aligned} \tag{4}$$

where a, b, c, d and d^* (with corresponding indexes) are coefficients of equations derived from matrices of stiffness, dissipation, and inertia; q_i is a generalized coordinate applied to the formation of the equation system; n is the number of generalized coordinates or DOFs; and η_1, η_2, η_3, η_4 are coordinates along which the car system is kinetically excited. More information about our model and its derivation can be found in [82]. The road profiles generated as above were used as input. When passing the corresponding profiles, the front and rear wheels were excited by road irregularities located at a distance equal to the distance between the axle centers.

The same ($h_{sF1} = h_{sF2} = h_{sR1} = h_{sR2}$), two different values for the front and rear ($h_{sF1} = h_{sF2}$, $h_{sR1} = h_{sR2}$), or all different damping coefficients (h_{sF1}, h_{sF2}, h_{sR1}, h_{sR2}) for all wheels, which define the behavior of the suspension, were optimized as parameters (marked as 1P, 2P, and 4P, respectively) to reach the minimal RMS value of the vertical acceleration of the crew. In other words, the suspension system was adjusted for the maximum driver, for the driver and front passenger, for the driver and rear left passenger, and for the entire crew comfort. The mathematical solution of Eq. (4) and the optimization process were processed using Simulink/MATLAB™ software and its response optimization, using the Gradient Descent method. The response optimization tool was configured to optimize the damping coefficients as parameters to find the minimum final value of the RMS of the vertical acceleration passing through the entire road profile. The objective function was constructed using the RMS value of the vertical acceleration for the driver, or their sum for the driver and front passenger, for the driver and rear left passenger, and for the entire crew, respectively, with default weighting value 1. All elements of the suspension system, tire stiffness, and damping were assumed to be linear [53]. During

optimization, the damping coefficient can vary from a minimum of 1000 Ns/m to a maximum of 15000 Ns/m. The masses of the crew were chosen as 100 kg, 80 kg, 60 kg, and 40 kg for the driver, front passenger, rear right passenger, and rear left passenger, respectively. The other parameters were the same as those used in Ref. [82].

3. Results and discussion

Initially, we generated road profiles with waviness w_1 values of 1, 2, 4, and 6; w_2 values of 0.5, 1, 2, and 3; and value of displacement PSD for ISO road class B $G_d(\Omega_0) = 4\times10^{-6}$ m^3 [79]. The length of the longitudinal road profile was 200 m. It is twice as much as needed to accommodate the ISO 8608 standard recommended the lower limits of the spatial frequency equal to 0.01 cycle/m. Using our dynamic full-car model, we had been simulating a vehicle passing these profiles at speeds $v = 20$, 50, 70, 90, and 130 km/h. When optimized for the driver and the same damping for all wheels, the values of the damping coefficient of the optimized suspension for the generated profiles and various speeds are shown in Table 1 and in Tables A1-A3, respectively, when optimized for the driver and front passenger, for the driver and rear left passenger, or for the whole crew.

Table 1. Dependence of the damping on vehicle speed and road waviness
(Cases: one coefficient (1P), optimization for driver $\left(\begin{smallmatrix}1&0\\0&0\end{smallmatrix}\right)$)

	Damping coefficients, Ns/m				
Waviness	20 km/h	50 km/h	70 km/h	90 km/h	130 km/h
$w_1 = 1; w_2 = 0.5$	1172	1242	1292	1216	1408
$w_1 = 2; w_2 = 0.5$	1169	1287	1605	1563	1771
$w_1 = 4; w_2 = 0.5$	1163	1506	2693	3053	2778
$w_1 = 6; w_2 = 0.5$	1152	2092	4991	6164	4127
$w_1 = 1; w_2 = 1$	1365	1448	1433	1279	1429
$w_1 = 2; w_2 = 1$	1360	1511	1786	1655	1793
$w_1 = 4; w_2 = 1$	1350	1800	2966	3207	2793
$w_1 = 6; w_2 = 1$	1334	2503	5476	6323	4131
$w_1 = 1; w_2 = 2$	1893	1926	1710	1396	1458
$w_1 = 2; w_2 = 2$	1878	2030	2121	1818	1818
$w_1 = 4; w_2 = 2$	1848	2462	3487	3452	2810
$w_1 = 6; w_2 = 2$	1807	3443	6426	6578	4142
$w_1 = 1; w_2 = 3$	2776	2462	1947	1487	1476
$w_1 = 2; w_2 = 3$	2726	2620	2418	1936	1835
$w_1 = 4; w_2 = 3$	2637	3211	3964	3630	2821
$w_1 = 6; w_2 = 3$	2545	4570	7330	6749	4148

The use of one damping value for all wheels in the full-car model was similar to the use of the quarter-car model. Nevertheless, the advantage is that we can optimize for different combinations of passenger positions and also consider pitch and roll dynamics and the influence of separate wheels. The dependencies of the optimized damping coefficient on the waviness w_1, w_2 and speed are the same as those observed to optimize suspensions with various locations of masses [74]. The optimal damping values increased when both waviness indices increased, except when the speed was equal to 20 km/h and w_1 increased. The highest damping values occurred when $w_1 = 6$ and the speed was 70 km/h or 90 km/h. Higher damping values are required to increase w_2 at a fixed w_1, and this difference changes from thousands to tens with increasing speed. When fixed w_2, the damping differences owing to the change in w_1 increased with increasing speed and reached a maximum at speeds of 70 km/h or 90 km/h. However, higher damping is also required when the optimization purpose is for the driver with the rear left passenger or whole crew compared to the optimization for the driver or for the driver with the front passenger. This is because rear suspensions require higher damping (see below).

Table 2. Dependence of the damping on vehicle speed and road waviness (Cases: two different coefficient for front and rear (2P), respectively, top and bottom values, optimization for driver and rear left passenger ($\begin{smallmatrix}1&0\\1&0\end{smallmatrix}$))

	Damping coefficients, Ns/m				
Waviness	20 km/h	50 km/h	70 km/h	90 km/h	130 km/h
$w_1 = 1; w_2 = 0.5$	1100 2444	1173 2164	1000 3426	1000 2770	1228 2570
$w_1 = 2; w_2 = 0.5$	1103 2404	1157 2746	1000 4976	1134 4610	1579 2786
$w_1 = 4; w_2 = 0.5$	1106 2335	1102 5165	1092 10022	1542 8163	2497 3451
$w_1 = 6; w_2 = 0.5$	1108 2251	1000 12291	1491 15000	3908 11078	3698 3833
$w_1 = 1; w_2 = 1$	1248 3117	1361 2702	1002 4029	1050 3193	1233 2740
$w_1 = 2; w_2 = 1$	1253 3067	1330 3536	1096 5713	1177 5091	1583 2949
$w_1 = 4; w_2 = 1$	1257 2942	1243 6680	1230 10460	1664 8287	2506 3513
$w_1 = 6; w_2 = 1$	1258 2839	1120 14389	1829 15000	4196 11168	3699 3847
$w_1 = 1; w_2 = 2$	1622 4842	1790 3991	1216 4948	1114 3871	1236 2948
$w_1 = 2; w_2 = 2$	1631 4768	1732 5223	1310 6675	1268 5619	1593 3135
$w_1 = 4; w_2 = 2$	1632 4555	1588 9283	1554 10918	1874 8428	2517 3580
$w_1 = 6; w_2 = 2$	1629 4254	1482 15000	2616 15000	4621 11279	3706 3857
$w_1 = 1; w_2 = 3$	2208 6880	2278 5115	1399 5525	1169 4284	1237 3060
$w_1 = 2; w_2 = 3$	2197 6731	2181 6521	1526 7199	1349 5931	1598 3213
$w_1 = 4; w_2 = 3$	2206 6528	1981 10891	1877 11132	2027 8506	2526 3608
$w_1 = 6; w_2 = 3$	2182 6080	1924 15000	3457 15000	4894 11323	3711 3863

A more realistic case in a vehicle is when different damping values are used for the front and rear suspensions. Such optimized results are presented in Table 2, optimizing for driver and rear left passenger or Tables A4-A6 optimizing for driver, driver and front passenger, and for the entire crew, respectively. Other results of more complex cases where all damping are different are shown in Table 3 optimizing for the whole crew or Tables A7-A9 optimizing for the driver, for the driver and front passenger, and for the driver and rear left passenger, respectively. The above-mentioned tendencies of dependencies of optimized damping are observed in cases with two and four different damping values with few peculiarities. Rear suspensions require higher damping values than front suspensions because of their larger share of total mass. The rear damping values do not increase but decrease with increasing waviness, but only if optimized for the driver or driver and front passenger (see Tables A4, A5, A7, A8). The highest damping values when $w_1 = 6$ shifted to a lower speed range (50 km/h or 70 km/h). There are situations where the limit damping values are reached, especially a lot of times when the speed is 50 km/h and 70 km/h and optimized for the driver or driver and front passenger. Here, one can observe the tendency that lower damping is required when the optimization purpose is the driver with rear left passenger or whole crew, compared with the optimization for the driver or for the driver with the front passenger (opposite to one damping value).

Table 3. Dependence of the damping on vehicle speed and road waviness (Cases: four different coefficients (4P) (top left is front left and bottom right is rear right), optimization for driver and all passengers ($\begin{smallmatrix}1 & 1\\ 1 & 1\end{smallmatrix}$))

	Damping coefficients, Ns/m									
Waviness	20 km/h		50 km/h		70 km/h		90 km/h		130 km/h	
$w_1 = 1; w_2 = 0.5$	1000	1068	1085	1123	1000	1000	1000	1000	1000	1319
	2400	3186	2213	2750	3539	4444	3004	3823	2282	4357
$w_1 = 2; w_2 = 0.5$	1000	1071	1033	1124	1000	1000	1000	1000	1000	1915
	2365	3146	2804	3645	5226	6592	5054	6373	2202	5508
$w_1 = 4; w_2 = 0.5$	1000	1076	1000	1040	1000	1000	1472	1183	1000	3581
	2294	3070	5694	6886	10129	11948	8304	8967	1940	6740
$w_1 = 6; w_2 = 0.5$	1000	1081	1000	1000	1314	1150	4725	1509	1789	5115
	2199	2966	13678	14830	15000	15000	10442	11128	2337	6190
$w_1 = 1; w_2 = 1$	1056	1243	1238	1316	1000	1000	1000	1000	1000	1325
	3087	4002	2852	3416	4336	5170	3598	4416	2420	4545
$w_1 = 2; w_2 = 1$	1058	1246	1196	1290	1000	1000	1000	1082	1000	1943
	3027	3941	3804	4532	6188	7450	5523	6794	2278	5639
$w_1 = 4; w_2 = 1$	1067	1247	1092	1188	1106	1008	1594	1285	1000	3607
	2938	3814	7719	8625	10690	12226	8451	8933	1942	6764
$w_1 = 6; w_2 = 1$	1071	1254	1000	1065	1596	1366	2512	5861	1815	5097
	2806	3675	15000	15000	15000	15000	12267	9470	2362	6198
$w_1 = 1; w_2 = 2$	1460	1575	1616	1784	1088	1109	1000	1013	1000	1322
	4894	5536	4567	4636	5577	6167	4514	5277	2621	4765
$w_1 = 2; w_2 = 2$	1456	1576	1550	1720	1158	1161	1106	1154	1000	1974
	4763	5417	6015	6112	7352	8209	6139	7139	2374	5777
$w_1 = 4; w_2 = 2$	1458	1580	1391	1554	1379	1325	1799	1501	1000	3634
	4583	5191	10687	10722	11269	11988	8637	8852	1945	6795
$w_1 = 6; w_2 = 2$	1463	1592	1356	1427	2323	2024	3128	5959	1843	5097
	4374	4980	15000	15000	15000	15000	12296	9603	2390	6197
$w_1 = 1; w_2 = 3$	2023	2243	2002	2410	1267	1298	1000	1124	1000	1321
	7139	7116	6168	5347	6307	6544	4959	5720	2740	4869
$w_1 = 2; w_2 = 3$	2033	2247	1914	2299	1366	1387	1200	1229	1000	1991
	6886	6925	7820	6932	7998	8376	6476	7276	2427	5842
$w_1 = 4; w_2 = 3$	2036	2215	1714	2054	1671	1690	1948	1704	1000	3647
	6604	6612	12652	11419	11734	11679	8750	8791	1947	6809
$w_1 = 6; w_2 = 3$	1997	2234	1809	1842	3156	2836	3529	6145	1860	5089
	6333	6281	15000	15000	15000	15000	12338	9680	2406	6197

More actual information is how all these changes influence ride comfort (in our case, the RMS of the vertical acceleration). We compared the RMS values on different sides of view to answer the question of what is the most suitable for ensuring the best ride comfort for all crews. First, we compared the percentage changes in the RMS value of vertical acceleration (for all four positions and the sum) relative to the reference of the corresponding RMS values of vertical acceleration for the corresponding speed and road profile when optimized for the driver. It was calculated as follows (using this equation, positive values indicate a percentage increase, whereas negative values indicate a percentage decrease):

$$\%\text{change} = \frac{\text{value} - \text{reference}}{\text{reference}} \times 100. \tag{5}$$

The maximum decrease and increase in the percentage change for the cases with one, two, or four damping coefficients and different optimizations are shown in Table 4 relative to the reference of the corresponding RMS values of vertical acceleration for the corresponding speed and road profile when optimized for the driver with the same number of damping values. The dependences of these reference values of the sum of the RMS value of the vertical accelerations

of the entire crew on the w_1 and w_2 waviness of the road profile when the vehicle speed is 20 km/h, 50 km/h, 70 km/h, 90 km/h, or 130 km/h are shown in Fig. 1 (or in Figs. A1-A4 for separate passengers). These dependencies of the reference values have the same common tendencies, and it is obvious that they have slightly different values. From the point of view of the optimization purpose relative to the optimization for the driver (Table 4), the sum of the RMS values decreased for all road profiles and speed values only if the optimization purpose was the entire crew using one, two, or four damping values as parameters (maximum down to –15 % or –0.58 m/s^2). However, for example, the percentage change of –13.7 % corresponds to –0.89 m/s^2 or –0.55 m/s^2 difference, or –7.36 % to –0.77 m/s^2. In general, there is no correlation between the values of percentage change and the values of difference (compare the results in Table 4 and Table A10 or Table A11 and Table A12), and the minimum and maximum values of difference and percentage change appear in different situations. A comparison of the dependences of the percentage change and difference on the road profile and speed for the two cases with the sum of the RMS is shown in Fig. 2. Only the zero values (blue lines in Fig. 2) were in the same location. Although the sum of the RMS values decreased for all road profiles and speed values when the optimization purpose was the entire crew using four damping values, a detailed analysis of the full data showed that the improvement in comfort is observed only for two or three passengers simultaneously, and it is one point ($w_1 = 1$, $w_2 = 1$, $v = 70$ km/h), where it improves for the driver. It is known from previous work [33], [74] that when changing the optimization purpose from only the driver to other purposes, we increase the comfort level for others but decrease it for the driver.

Table 4. The maximum percentage change in the RMS value of vertical acceleration (for the four positions and the sum) relative to the reference of the corresponding RMS values of vertical acceleration for the corresponding speed and road profile when optimized for the driver with the same number of damping values. FL – front left (driver), FR – front right passenger, RL – rear left passenger, RR – rear right passenger

Damping values			Percentage change, %				
	Optimized for		RMS(a_{FL})	RMS(a_{FR})	RMS(a_{RR})	RMS(a_{RL})	ΣRMS
1P	$\begin{pmatrix}1&0\\0&0\end{pmatrix}$	as reference					
	$\begin{pmatrix}1&1\\0&0\end{pmatrix}$	min	0.00	–0.69	–0.90	–0.89	–0.51
		max	0.26	0.00	2.55	2.28	1.08
	$\begin{pmatrix}1&0\\1&0\end{pmatrix}$	min	0.02	–0.24	–19.9	–18.7	–6.88
		max	9.06	8.31	–0.03	–0.04	0.09
	$\begin{pmatrix}1&1\\1&1\end{pmatrix}$	min	0.01	-0.36	–20.7	–19.5	–6.90
		max	10.1	9.20	0.14	0.10	–0.00
2P	$\begin{pmatrix}1&0\\0&0\end{pmatrix}$	as reference					
	$\begin{pmatrix}1&1\\0&0\end{pmatrix}$	min	–0.69	–2.55	–8.66	–8.21	–5.39
		max	0.52	0.00	1.73	1.98	0.81
	$\begin{pmatrix}1&0\\1&0\end{pmatrix}$	min	–0.24	–0.06	–33.7	–34.4	–14.9
		max	14.1	12.6	–0.18	–0.28	0.09
	$\begin{pmatrix}1&1\\1&1\end{pmatrix}$	min	–0.30	–0.15	–33.2	–33.9	–15.1
		max	14.1	12.0	0.02	–0.04	–0.01
4P	$\begin{pmatrix}1&0\\0&0\end{pmatrix}$	as reference					
	$\begin{pmatrix}1&1\\0&0\end{pmatrix}$	min	–1.05	–24.2	–15.6	–7.58	–7.36
		max	11.9	0.06	23.2	11.0	3.95
	$\begin{pmatrix}1&0\\1&0\end{pmatrix}$	min	–0.01	–17.5	–29.9	–35.8	–13.7
		max	27.9	31.7	16.6	–1.13	4.76
	$\begin{pmatrix}1&1\\1&1\end{pmatrix}$	min	–0.00	–18.5	–31.7	–32.8	–13.7
		max	10.5	10.7	4.92	3.64	–0.00

The dependence of the difference in the RMS value of the vertical acceleration of the separate passengers on the w_1 and w_2 waviness of the road profile and vehicle speed is shown in Fig. 3 for the case optimized for the entire crew with four damping values relative to the reference when

optimized for the driver with four damping values. In all calculated situations, there are only a few situations where comfort is improved for the entire crew (see Table 5) compared to optimization for the driver. Most of them occur when we change the optimization purpose from the driver to the driver with the front-right passenger. The highest increases in comfort for separate passengers are from 30 % to 36 % for rear passengers when optimized for the driver and rear left passenger or for the entire crew with two or four damping values (RMS values decrease in the range from –0.35 m/s^2 to –1 m/s^2).

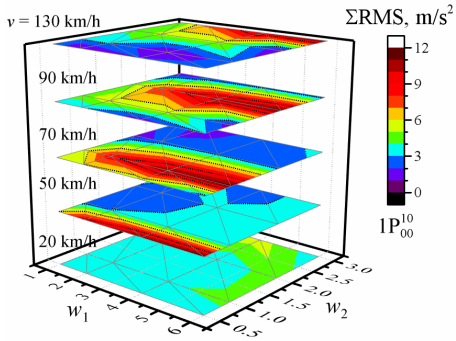

a) Optimized for the driver with one damping value

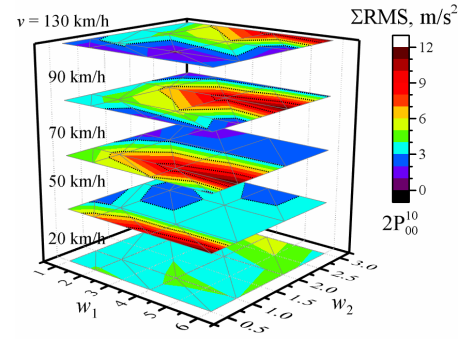

b) Optimized for the driver with two damping values

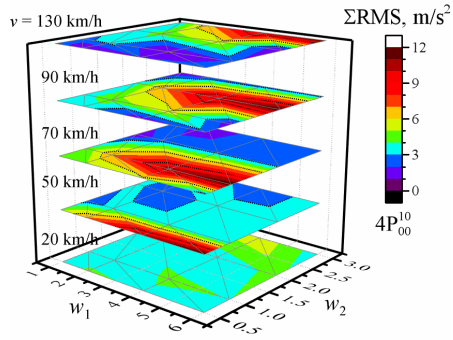

c) Optimized for the driver with four damping values

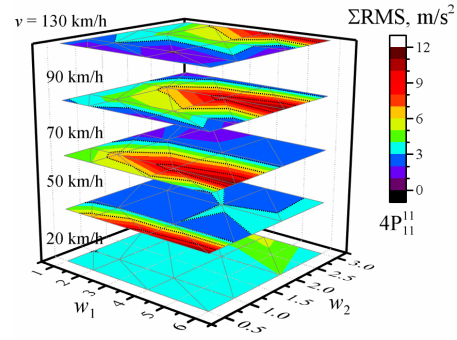

d) Optimized for the entire crew with four damping values

Fig. 1. Dependence of the sum of the RMS values of the vertical accelerations of the entire crew on the w_1 and w_2 waviness of the road profile and the vehicle speed v. The black dotted line shows the major tick value

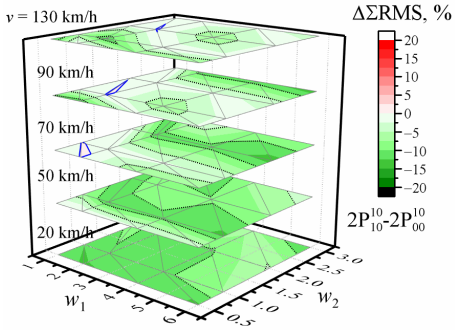

a) Optimized for the driver and rear left passenger with two damping values

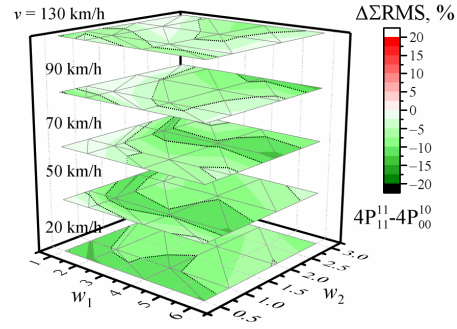

b) Optimized for the entire crew with four damping values

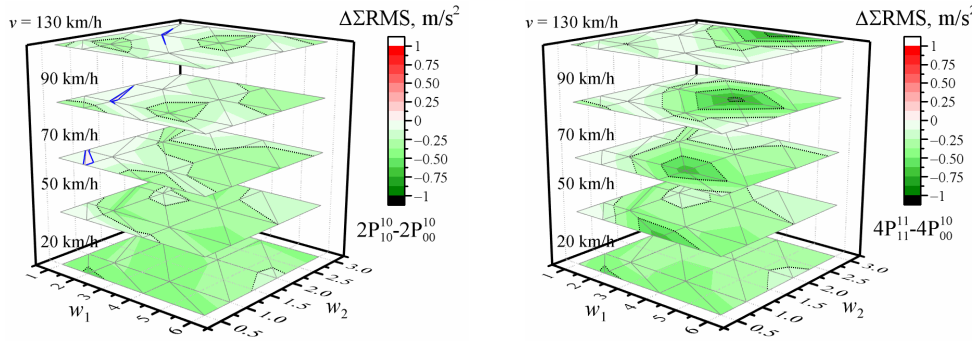

c) Optimized for the driver and rear left passenger with two damping values

d) Optimized for the entire crew with four damping values

Fig. 2. Dependence of the percentage change (a, b) / difference (c, d) in the sum of the RMS values of vertical accelerations of the entire crew on the w_1 and w_2 waviness of the road profile and the vehicle speed v relative to the reference of the corresponding sum of the RMS values of vertical accelerations for the corresponding speed and road profile when optimized for the driver, respectively, with two or four damping values. The black dotted line shows the major tick value. The solid blue line is zero

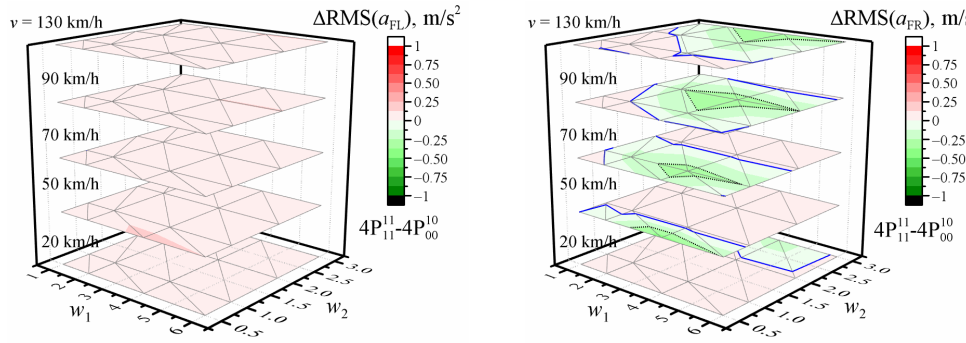

a) Of the driver (front left)

b) Of the front right passenger

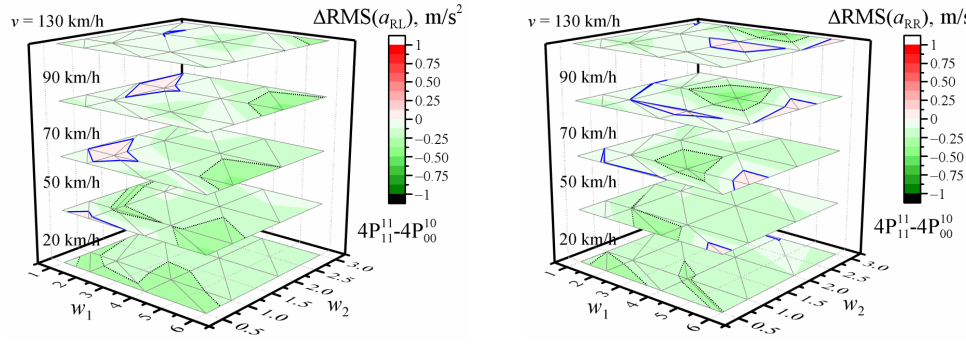

c) Of the rear left passenger

d) Of the rear right passenger

Fig. 3. Dependence of the difference in the RMS value of the vertical acceleration (a, b, c, d) on the w_1 and w_2 waviness of the road profile and the vehicle speed v when optimized for the entire crew with four damping values relative to the reference of the corresponding RMS values of vertical accelerations for the corresponding speed and road profile when optimized for the driver with four damping values. The black dotted line shows the major tick value. The solid blue line is zero

The comparison results relative to the optimization for the entire crew with four damping values are presented in Table 6. Here, we show the average percentage change over all profiles and velocities. From these results, we can state that the optimization for the entire crew with only four damping values is not the best choice for all passengers in all cases. Negligible changes in

ISSN PRINT 1392-8716, ISSN ONLINE 2538-8460

the increase and decrease in the sum of the RMS were obtained when optimized for the driver and rear left passenger or the entire crew with two damping values compared with the case of the entire crew with four damping values (see Table A11). These three cases had nearly the same average sum of the RMS averaged over all profiles and velocities.

Table 5. Points where comfort increases for the entire crew relative to the reference when optimized for the driver with the same number of damping values

Cases	w_1	w_2	v, km/h	ΔΣRMS, m/s^2	ΔΣ RMS, %
$4P_{00}^{11} - 4P_{00}^{10}$	1	2	50	–0.00011	–0.0033
	1	3	50	–0.140	–3.9
	6	2	70	–0.00014	–0.0049
	1	0.5	90	–0.137	–4.3
$2P_{11}^{11} - 2P_{00}^{10}$	6	2	130	–0.014	–1.7
$2P_{10}^{10} - 2P_{00}^{10}$	6	2	130	–0.014	–1.7
$2P_{00}^{11} - 2P_{00}^{10}$	1	2	20	–0.147	–3.7
	6	3	20	–0.017	–0.48
	1	3	50	–0.14	–4.1
	2	3	50	–0.21	–5.4
	1	3	70	–0.00032	–0.01
	1	0.5	90	-0.14	–4.4
	2	0.5	130	–0.0006	–0.078
	6	2	130	–0.0026	–0.3

Fig. 4 shows the dependence of the difference in the RMS value of the vertical accelerations on the waviness w_1 and w_2 of the road profile and the vehicle speed when optimized for the entire crew with four damping values relative to the reference of the corresponding RMS values of the vertical accelerations for the corresponding speed and road profile when optimized for the entire crew with two damping values. It can be seen that only for the driver is better optimization with four damping values. This could be explained by the fact that, when optimized for the entire crew with four damping values, we sometimes reached the limit values. We believe that better comfort results will be obtained if during optimization 1) we would check the minimal value separately for all passengers; 2) we would change not only damping, but also stiffness, or would use asymmetric suspensions or non-linear models; and 3) we would limit the highest values of acceleration. The comfort level is very low when the magnitude of the total values of the overall vibration ranges from 1.25 m/s^2 to 2.5 m/s^2 and extremely uncomfortable when they are even greater [66]. When the acceleration value is still high even after optimization, we could also additionally recommend reducing the speed. Therefore, by combining information from vehicle sensors about speed, masses with their location and information stored in a microcomputer or cloud about optimal damping, vertical acceleration, and road information, we can control damping and recommend or reduce driving speed [83], [84]. Using real-time data, the required damping value could be interpolated from 3D lookup tables of optimized damping coefficients calculated at our fixed values of speed v and waviness indices w_1, w_2 by applying different optimization strategies.

Comparing our four optimization tasks, we can conclude that optimization for the driver and for the driver and front-right passenger gives similar results with one damping value. However, the percentage change increases with an increasing number of damping values. When comparing the optimization for the driver and rear-left passenger and for the entire crew, one has nearly similar values, except for the case with four damping values, where the larger changes are. This could be related to the higher comfort level of the crew. Finally, we could recommend to use one damping value when the speed of calculation is required for a short time (e.g., detected bump on the road). Add more regimes, for example, ‘taxi,’ when optimized for the driver because he rides all day and the passengers only ride for a short time, or ‘trip’ when optimized for the entire crew.

Table 6. The average over all profiles and velocities of percentage change in the RMS value of vertical acceleration (for all four positions and the sum) relative to the reference of the corresponding RMS values of vertical acceleration for the corresponding speed and road profile when optimized for the entire crew $\binom{1\ 1}{1\ 1}$ with four damping values (4P). FL – front left (driver), FR – front right passenger, RL – rear left passenger, RR – rear right passenger

Damping values		Average of percentage change, %				
	Optimized for	RMS(a_{FL})	RMS(a_{FR})	RMS(a_{RR})	RMS(a_{RL})	ΣRMS
1P	$\binom{1\ 0}{0\ 0}$	16.1	12.3	12.1	7.08	11.7
	$\binom{1\ 1}{0\ 0}$	16.2	12.1	12.6	7.56	11.9
	$\binom{1\ 0}{1\ 0}$	19.6	15.8	3.55	–0.82	9.10
	$\binom{1\ 1}{1\ 1}$	19.9	15.9	3.41	–0.95	9.09
2P	$\binom{1\ 0}{0\ 0}$	–1.44	–4.89	20.0	19.0	6.95
	$\binom{1\ 1}{0\ 0}$	–1.38	–5.18	19.5	18.6	6.64
	$\binom{1\ 0}{1\ 0}$	3.83	–0.05	–0.56	–2.65	0.01
	$\binom{1\ 1}{1\ 1}$	3.40	–0.84	–0.15	–2.08	–0.06
4P	$\binom{1\ 0}{0\ 0}$	–4.09	0.51	17.6	18.0	7.01
	$\binom{1\ 1}{0\ 0}$	–2.34	–4.76	18.8	18.8	6.50
	$\binom{1\ 0}{1\ 0}$	2.13	5.42	3.35	–4.10	1.49
	$\binom{1\ 1}{1\ 1}$	As reference				

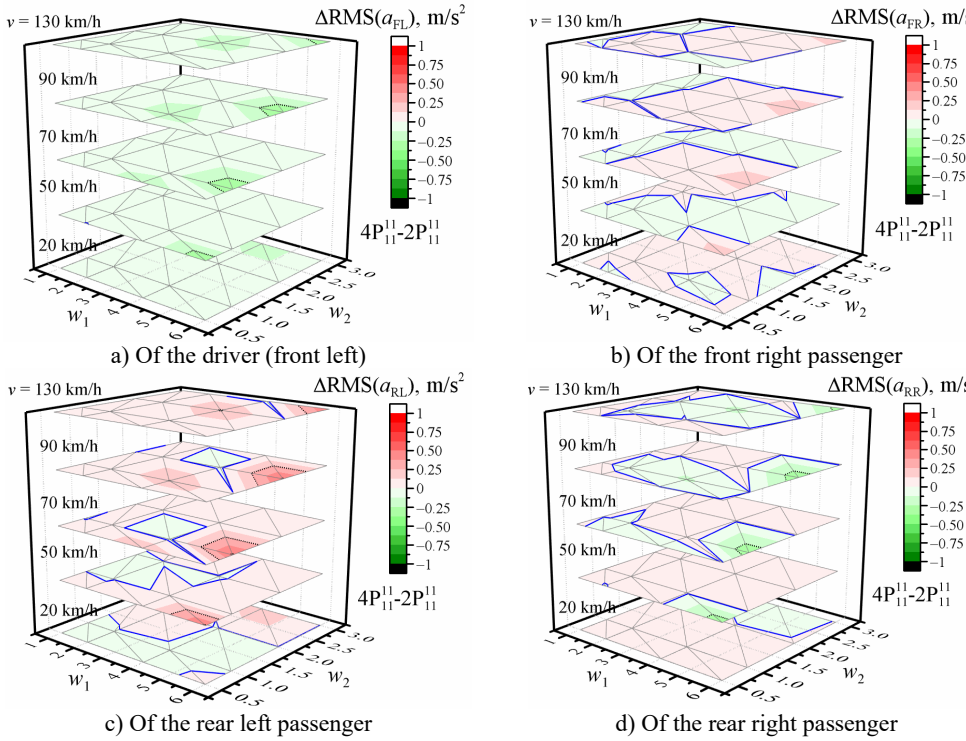

Fig. 4. Dependence of the difference in the RMS value of the vertical acceleration (a, b, c, d) on the w_1 and w_2 waviness of the road profile and the vehicle speed v when optimized for the entire crew with four damping values relative to the reference of the corresponding RMS values of vertical accelerations for the corresponding speed and road profile when optimized for the entire crew with two damping values. The black dotted line shows the major tick value. The solid blue line is zero

4. Conclusions

The relationship between the detected road waviness values and optimized damping

coefficient can be used to control the damping of the suspension system and recommend or reduce the driving speed. The required optimized damping value could be interpolated from a 3D gridded matrix of damping coefficients calculated at certain fixed values of speed and waviness indices when optimized with the same, two different for the front and rear, or all different damping coefficients for all wheels and using different optimization strategies. Our simulation results showed that higher damping is required when the optimization purpose is for the driver with the rear left passenger or the entire crew compared to the optimization for the driver or for the driver with the front passenger. In addition, optimization by changing only two or four different damping coefficients in the suspension system is not sufficient because there are too many cases where it reaches limit values.

From the point of view of the optimization purpose relative to the optimization for the driver, the sum of the RMS values decreases for all road profiles and speed values only if the optimization purpose is the entire crew using one, two, or four damping values as parameters (maximum down to –15 %). Comparing the optimization for the driver and rear-left passenger and for the entire crew, we obtained similar values, except for the case with four damping values, where larger changes were observed. However, the optimization for the entire crew with four damping values is not the best choice for all situations. Furthermore, we could recommend two regimes like 'taxi' and 'trip' where the comfort level is optimized for the driver or the entire crew, respectively.

For future improvement, we believe that better results will be obtained if 1) we would change not only damping but also stiffness or would use asymmetric suspensions or nonlinear models; 2) we would check the minimal value separately for all passengers during optimization; and 3) we would control the highest values of acceleration reducing speed.

Acknowledgements

The authors have not disclosed any funding.

Data availability

The datasets generated during and/or analyzed during the current study are available from the corresponding author on reasonable request.

Author contributions

Aurimas Čerškus: conceptualization, methodology, validation, formal analysis, investigation, data curation, writing-original draft preparation, writing-review and editing. Nikolaj Šešok: methodology, software, validation, investigation, resources, visualization. Vytautas Bučinskas: conceptualization, writing-review and editing, supervision

Conflict of interest

The authors declare that they have no conflict of interest.

References

[1] P. S. Els, N. J. Theron, P. E. Uys, and M. J. Thoresson, "The ride comfort vs. handling compromise for off-road vehicles," *Journal of Terramechanics*, Vol. 44, No. 4, pp. 303–317, Oct. 2007, https://doi.org/10.1016/j.jterra.2007.05.001

[2] J. Zhu, W. Zhang, and M. X. Wu, "Evaluation of ride comfort and driving safety for moving vehicles on slender coastal bridges," *Journal of Vibration and Acoustics*, Vol. 140, No. 5, p. 05101, Oct. 2018, https://doi.org/10.1115/1.4039569

[3] T. Li, *Vehicle/Tire/Road Dynamics: Handling, Ride, and NVH*. Elsevier, 2022.

[4] D. Karnopp, "Active damping in road vehicle suspension systems," *Vehicle System Dynamics*, Vol. 12, No. 6, pp. 291–311, Jul. 2007, https://doi.org/10.1080/00423118308968758

[5] R. S. Sharp and D. A. Crolla, "Road vehicle suspension system design – a review," *Vehicle System Dynamics*, Vol. 16, No. 3, pp. 167–192, Jan. 1987, https://doi.org/10.1080/00423118708968877

[6] D. Fischer and R. Isermann, "Mechatronic semi-active and active vehicle suspensions," *Control Engineering Practice*, Vol. 12, No. 11, pp. 1353–1367, Nov. 2004, https://doi.org/10.1016/j.conengprac.2003.08.003

[7] Z. Lozia, "The use of a linear quarter-car model to optimize the damping in a passive automotive suspension system – a follow-on from many authors' works of the recent 40 years," *The Archives of Automotive Engineering – Archiwum Motoryzacji*, Vol. 71, No. 1, pp. 39–71, Mar. 2016, https://doi.org/10.14669/am.vol71.art3

[8] J. Goszczak, G. Mitukiewicz, B. Radzymiński, A. Werner, T. Szydłowski, and D. Batory, "The study of damping control in semi-active car suspension," *Journal of Vibroengineering*, Vol. 22, No. 4, pp. 933–944, Jun. 2020, https://doi.org/10.21595/jve.2020.20578

[9] S. Tengler and K. Warwas, "Driver comfort improvement by a selection of optimal springing of a seat," *Czasopismo Techniczne*, Vol. 5, pp. 217–235, Jan. 2017, https://doi.org/10.4467/2353737xct.17.083.6440

[10] J. K. Nkrumah, K. S. Amedorme, B. Ziblim, and D. I. Offei, "Review of suspension control and simulation of passive, semi-active and active suspension systems using quarter vehicle model," *American Scientific Research Journal for Engineering, Technology, and Sciences*, Vol. 90, No. 1, pp. 144–160, Oct. 2022.

[11] P. Barak, "Passive versus active and semi-active suspension from theory to application in north American industry," SAE Technical Paper 922140, Sep. 1992.

[12] I. Ballo, "Comparison of the properties of active and semiactive suspension," *Vehicle System Dynamics*, Vol. 45, No. 11, pp. 1065–1073, Nov. 2007, https://doi.org/10.1080/00423110701191575

[13] G. Z. Yao, F. F. Yap, G. Chen, W. H. Li, and S. H. Yeo, "MR damper and its application for semi-active control of vehicle suspension system," *Mechatronics*, Vol. 12, No. 7, pp. 963–973, Sep. 2002, https://doi.org/10.1016/s0957-4158(01)00032-0

[14] D. Karnopp, M. J. Crosby, and R. A. Harwood, "Vibration control using semi-active force generators," *Journal of Engineering for Industry*, Vol. 96, No. 2, pp. 619–626, May 1974, https://doi.org/10.1115/1.3438373

[15] J. Swevers, C. Lauwerys, B. Vandersmissen, M. Maes, K. Reybrouck, and P. Sas, "A model-free control structure for the on-line tuning of the semi-active suspension of a passenger car," *Mechanical Systems and Signal Processing*, Vol. 21, No. 3, pp. 1422–1436, Apr. 2007, https://doi.org/10.1016/j.ymssp.2006.05.005

[16] D. Savaresi, F. Favalli, S. Formentin, and S. M. Savaresi, "On-line damping estimation in road vehicle semi-active suspension systems," *IFAC-PapersOnLine*, Vol. 52, No. 5, pp. 679–684, Jan. 2019, https://doi.org/10.1016/j.ifacol.2019.09.108

[17] S. Lajqi and S. Pehan, "Designs and optimizations of active and semi-active non-linear suspension systems for a terrain vehicle," *Strojniški vestnik – Journal of Mechanical Engineering*, Vol. 58, No. 12, pp. 732–743, Dec. 2012, https://doi.org/10.5545/sv-jme.2012.776

[18] N. Zhang and Q. Zhao, "Fuzzy sliding mode controller design for semi-active seat suspension with neuro-inverse dynamics approximation for MR damper," *Journal of Vibroengineering*, Vol. 19, No. 5, pp. 3488–3511, Aug. 2017, https://doi.org/10.21595/jve.2017.17654

[19] L. Z. Ben, F. Hasbullah, and F. W. Faris, "A comparative ride performance of passive, semi-active and active suspension systems for off-road vehicles using half car model," *International Journal of Heavy Vehicle Systems*, Vol. 21, No. 1, p. 26, Jan. 2014, https://doi.org/10.1504/ijhvs.2014.057827

[20] P. Krauze, "Comparison of control strategies in a semi-active suspension system of the experimental ATV," *Journal of Low Frequency Noise, Vibration and Active Control*, Vol. 32, No. 1-2, pp. 67–80, Mar. 2013, https://doi.org/10.1260/0263-0923.32.1-2.67

[21] E. M. Elbeheiry and D. C. Karnopp, "Optimization of active and passive suspensions based on a full car model," *International Congress and Exposition*, Vol. 104, pp. 1900–1911, Feb. 1995, https://doi.org/10.4271/951063

[22] J. Qiao, Y. Choi, and F. Yang, "PSO optimum control strategy of 7 degrees of freedom semi-active suspensions," *Journal of Mechanical Engineering, Automation and Control Systems*, Vol. 2, No. 2, pp. 98–108, Dec. 2021, https://doi.org/10.21595/jmeacs.2021.22164

[23] S. Chen, H. Chen, and D. Negrut, "Implementation of MPC-based path tracking for autonomous vehicles considering three vehicle dynamics models with different fidelities," *Automotive Innovation*, Vol. 3, No. 4, pp. 386–399, Dec. 2020, https://doi.org/10.1007/s42154-020-00118-w

[24] S. H. Zareh, A. Sarrafan, A. A. A. Khayyat, and A. Zabihollah, "Intelligent semi-active vibration control of eleven degrees of freedom suspension system using magnetorheological dampers," *Journal of Mechanical Science and Technology*, Vol. 26, No. 2, pp. 323–334, Apr. 2012, https://doi.org/10.1007/s12206-011-1007-6

[25] S. H. Zareh, M. Abbasi, H. Mahdavi, and K. G. Osgouie, "Semi-active vibration control of an eleven degrees of freedom suspension system using neuro inverse model of magnetorheological dampers," *Journal of Mechanical Science and Technology*, Vol. 26, No. 8, pp. 2459–2467, Aug. 2012, https://doi.org/10.1007/s12206-012-0628-8

[26] S. Kopylov, Z. Chen, and M. A. A. Abdelkareem, "Implementation of an electromagnetic regenerative tuned mass damper in a vehicle suspension system," *IEEE Access*, Vol. 8, pp. 110153–110163, Jan. 2020, https://doi.org/10.1109/access.2020.3002275

[27] G. G. Fossati, L. F. F. Miguel, and W. J. P. Casas, "Multi-objective optimization of the suspension system parameters of a full vehicle model," *Optimization and Engineering*, Vol. 20, No. 1, pp. 151–177, Sep. 2018, https://doi.org/10.1007/s11081-018-9403-8

[28] D. Joshi and A. Deb, "Effect of sitting occupancy on lateral dynamics and trajectory of a passenger car," in *ASME 2015 International Design Engineering Technical Conferences and Computers and Information in Engineering Conference*, Vol. 6, Aug. 2015, https://doi.org/10.1115/detc2015-47528

[29] A. Deb and D. Joshi, "A study on ride comfort assessment of multiple occupants using lumped parameter analysis," in *SAE 2012 World Congress and Exhibition*, Apr. 2012, https://doi.org/10.4271/2012-01-0053

[30] H. Du, W. Li, and N. Zhang, "Semi-active control of an integrated full-car suspension with seat suspension and driver body model using ER dampers," *International Journal of Vehicle Design*, Vol. 63, No. 2/3, p. 159, Jan. 2013, https://doi.org/10.1504/ijvd.2013.056133

[31] V. Guruguntla and M. Lal, "Multi-body modelling and ride comfort analysis of a seated occupant under whole-body vibration," *Journal of Vibration and Control*, Vol. 29, No. 13-14, pp. 3078–3095, May 2022, https://doi.org/10.1177/10775463221091089

[32] D. Joshi, A. Deb, and C. Chou, "A study on combined effects of road roughness, vehicle velocity and sitting occupancies on multi-occupant vehicle ride comfort assessment," *WCX™ 17: SAE World Congress Experience*, Mar. 2017, https://doi.org/10.4271/2017-01-0409

[33] P. E. Uys, P. S. Els, and M. Thoresson, "Suspension settings for optimal ride comfort of off-road vehicles travelling on roads with different roughness and speeds," *Journal of Terramechanics*, Vol. 44, No. 2, pp. 163–175, Apr. 2007, https://doi.org/10.1016/j.jterra.2006.05.002

[34] A. J. Nieto, A. L. Morales, J. M. Chicharro, and P. Pintado, "An adaptive pneumatic suspension system for improving ride comfort and handling," *Journal of Vibration and Control*, Vol. 22, No. 6, pp. 1492–1503, Jun. 2014, https://doi.org/10.1177/1077546314539717

[35] A. L. Morales, A. J. Nieto, J. M. Chicharro, and P. Pintado, "A semi-active vehicle suspension based on pneumatic springs and magnetorheological dampers," *Journal of Vibration and Control*, Vol. 24, No. 4, pp. 808–821, Jun. 2016, https://doi.org/10.1177/1077546316653004

[36] A. Hać, "Optimal linear preview control of active vehicle suspension," *Vehicle System Dynamics*, Vol. 21, No. 1, pp. 167–195, Jan. 1992, https://doi.org/10.1080/00423119208969008

[37] I. Youn and A. Hać, "Semi-active suspensions with adaptive capability," *Journal of Sound and Vibration*, Vol. 180, No. 3, pp. 475–492, Feb. 1995, https://doi.org/10.1006/jsvi.1995.0091

[38] T.-H. Wu and C.-C. Lan, "A wide-range variable stiffness mechanism for semi-active vibration systems," *Journal of Sound and Vibration*, Vol. 363, pp. 18–32, Feb. 2016, https://doi.org/10.1016/j.jsv.2015.10.024

[39] R. Tchamna, M. Lee, and I. Youn, "Attitude control of full vehicle using variable stiffness suspension control," *Optimal Control Applications and Methods*, Vol. 36, No. 6, pp. 936–952, Nov. 2014, https://doi.org/10.1002/oca.2149

[40] C. Spelta et al., "Performance analysis of semi-active suspensions with control of variable damping and stiffness," *Vehicle System Dynamics*, Vol. 49, No. 1-2, pp. 237–256, Feb. 2011, https://doi.org/10.1080/00423110903410526

[41] V. Goga and M. Kľúčik, "Optimization of vehicle suspension parameters with use of evolutionary computation," *Procedia Engineering*, Vol. 48, pp. 174–179, Jan. 2012, https://doi.org/10.1016/j.proeng.2012.09.502

[42] R. Jayachandran and S. Krishnapillai, "Modeling and optimization of passive and semi-active suspension systems for passenger cars to improve ride comfort and isolate engine vibration," *Journal*

of Vibration and Control, Vol. 19, No. 10, pp. 1471–1479, May 2012, https://doi.org/10.1177/1077546312445199

[43] H. Huang, S. Sun, S. Chen, and W. Li, "Numerical and experimental studies on a new variable stiffness and damping magnetorheological fluid damper," *Journal of Intelligent Material Systems and Structures*, Vol. 30, No. 11, pp. 1639–1652, Apr. 2019, https://doi.org/10.1177/1045389x19844003

[44] J. Kumar and G. Bhushan, "Dynamic analysis of quarter car model with semi-active suspension based on combination of magneto-rheological materials," *International Journal of Dynamics and Control*, Vol. 11, No. 2, pp. 482–490, Aug. 2022, https://doi.org/10.1007/s40435-022-01024-1

[45] A. Soliman and M. Kaldas, "Semi-active suspension systems from research to mass-market – A review," *Journal of Low Frequency Noise, Vibration and Active Control*, Vol. 40, No. 2, pp. 1005–1023, Oct. 2019, https://doi.org/10.1177/1461348419876392

[46] S. M. Savaresi, C. Poussot-Vassal, C. Spelta, O. Sename, and L. Dugard, *Semi-Active Suspension Control Design for Vehicles*. Elsevier, 2010, https://doi.org/10.1016/c2009-0-63839-3

[47] P. Brezas, M. C. Smith, and W. Hoult, "A clipped-optimal control algorithm for semi-active vehicle suspensions: Theory and experimental evaluation," *Automatica*, Vol. 53, pp. 188–194, Mar. 2015, https://doi.org/10.1016/j.automatica.2014.12.026

[48] E. Guglielmino, T. Sireteanu, C. W. Stammers, G. Gheorghe, and M. Giuclea, "Semi-active control algorithms," in *Semi-active Suspension Control*, London: Springer London, 2024, pp. 65–97, https://doi.org/10.1007/978-1-84800-231-9_4

[49] C. Lin, W. Liu, and H. Ren, "State estimation based on unscented Kalman filter for semi-active suspension systems," *Journal of Vibroengineering*, Vol. 18, No. 1, pp. 446–457, Feb. 2016.

[50] S. Ni and V. Nguyen, "Performance of semi-active cab suspension system with different control methods," *Journal of Mechatronics and Artificial Intelligence in Engineering*, Vol. 4, No. 1, pp. 8–17, Jun. 2023, https://doi.org/10.21595/jmai.2022.23019

[51] C. Lauwerys, J. Swevers, and P. Sas, "Robust linear control of an active suspension on a quarter car test-rig," *Control Engineering Practice*, Vol. 13, No. 5, pp. 577–586, May 2005, https://doi.org/10.1016/j.conengprac.2004.04.018

[52] R. Hirao, K. Kasuya, and N. Ichimaru, "A semi-active suspension system using ride control based on bi-linear optimal control theory and handling control considering roll feeling," *SAE 2015 World Congress and Exhibition*, Apr. 2015, https://doi.org/10.4271/2015-01-1501

[53] I. Ahmad and A. Khan, "A comparative analysis of linear and nonlinear semi-active suspension system," *Mehran University Research Journal of Engineering and Technology*, Vol. 37, No. 2, pp. 233–240, Apr. 2018, https://doi.org/10.22581/muet1982.1802.01

[54] A. G. Mohite and A. C. Mitra, "Development of linear and non-linear vehicle suspension model," *Materials Today: Proceedings*, Vol. 5, No. 2, pp. 4317–4326, Jan. 2018, https://doi.org/10.1016/j.matpr.2017.11.697

[55] D. N. L. Horton and D. A. Crolla, "Theoretical analysis of a semi active suspension fitted to an off-road vehicle," *Vehicle System Dynamics*, Vol. 15, No. 6, pp. 351–372, Jul. 2007, https://doi.org/10.1080/00423118608968860

[56] E. Palomares, J. C. Bellido, A. L. Morales, A. J. Nieto, J. M. Chicharro, and P. Pintado, "Pointwise-constrained optimal control of a semiactive vehicle suspension," *Optimal Control Applications and Methods*, Vol. 42, No. 1, pp. 216–235, Sep. 2020, https://doi.org/10.1002/oca.2671

[57] A. Giua, M. Melas, C. Seatzu, and G. Usai, "Design of a predictive semiactive suspension system," *Vehicle System Dynamics*, Vol. 41, No. 4, pp. 277–300, Apr. 2004, https://doi.org/10.1080/00423110412331315169

[58] G. Li, Z. Ruan, R. Gu, and G. Hu, "Fuzzy sliding mode control of vehicle magnetorheological semi-active air suspension," *Applied Sciences*, Vol. 11, No. 22, p. 10925, Nov. 2021, https://doi.org/10.3390/app112210925

[59] L. L. Zhao, C. C. Zhou, and Y. W. Yu, "A research on optimal damping ratio control strategy for semi-active suspension system," *Automot. Eng.*, Vol. 40, No. 2018, pp. 41–47, 2018.

[60] A. Hac´ and I. Youn, "Optimal semi-active suspension with preview based on a quarter car model," *Journal of Vibration and Acoustics*, Vol. 114, No. 1, pp. 84–92, Jan. 1992, https://doi.org/10.1115/1.2930239

[61] J. Theunissen, A. Tota, P. Gruber, M. Dhaens, and A. Sorniotti, "Preview-based techniques for vehicle suspension control: a state-of-the-art review," *Annual Reviews in Control*, Vol. 51, pp. 206–235, Jan. 2021, https://doi.org/10.1016/j.arcontrol.2021.03.010

[62] M. W. Sayers, T. D. Gillespie, and C. A. V. Queiroz, *International Road Roughness Experiment: a Basis for Establishing a Standard Scale for Road Roughness Measurements*. Washington, D.C.: World Bank, 1986.

[63] M. W. Sayers and S. M. Karamihas, *The Little Book of Profiling-Basic Information about Measuring and Interpreting Road Profile*. New York, NY, USA: Regent of the University of Michigan, 1998.

[64] G. Loprencipe and G. Cantisani, "Unified analysis of road pavement profiles for evaluation of surface characteristics," *Modern Applied Science*, Vol. 7, No. 8, pp. 1–14, Jul. 2013, https://doi.org/10.5539/mas.v7n8p1

[65] T. Nguyen, B. Lechner, and Y. D. Wong, "Response-based methods to measure road surface irregularity: a state-of-the-art review," *European Transport Research Review*, Vol. 11, No. 1, p. 43, Oct. 2019, https://doi.org/10.1186/s12544-019-0380-6

[66] "Mechanical vibration and shock – Evaluation of human exposure to whole-body vibration – Part 1: General requirements," International Organization for Standardization, ISO 2631-1:1997, Jan. 1997.

[67] G. Guastadisegni et al., "Ride analysis tools for passenger cars: objective and subjective evaluation techniques and correlation processes – a review," *Vehicle System Dynamics*, Vol. 62, No. 7, pp. 1876–1902, Jul. 2024, https://doi.org/10.1080/00423114.2023.2259024

[68] G. Papaioannou and D. Koulocheris, "An approach for minimizing the number of objective functions in the optimization of vehicle suspension systems," *Journal of Sound and Vibration*, Vol. 435, pp. 149–169, Nov. 2018, https://doi.org/10.1016/j.jsv.2018.08.009

[69] Z. Lozia and P. Zdanowicz, "Optimization of damping in the passive automotive suspension system with using two quarter-car models," in *IOP Conference Series: Materials Science and Engineering*, Vol. 148, No. 1, p. 012014, Sep. 2016, https://doi.org/10.1088/1757-899x/148/1/012014

[70] S. A. Abu Bakar, P. M. Samin, H. Jamaluddin, R. A. Rahman, and S. Sulaiman, "Semi active suspension system performance under random road profile excitations," in *International Conference on Computer, Communications, and Control Technology (I4CT)*, pp. 93–97, Apr. 2015, https://doi.org/10.1109/i4ct.2015.7219544

[71] T. Lenkutis, D. Viržonis, A. Čerškus, A. Dzedzickis, N. Šešok, and V. Bučinskas, "An automotive ferrofluidic electromagnetic system for energy harvesting and adaptive damping," *Sensors*, Vol. 22, No. 3, p. 1195, Feb. 2022, https://doi.org/10.3390/s22031195

[72] T. Lenkutis et al., "Extraction of information from a PSD for the control of vehicle suspension," in *Automation 2021: Recent Achievements in Automation, Robotics and Measurement Techniques*, pp. 146–153, Apr. 2021, https://doi.org/10.1007/978-3-030-74893-7_15

[73] A. Čerškus, T. Lenkutis, N. Šešok, A. Dzedzickis, D. Viržonis, and V. Bučinskas, "Identification of road profile parameters from vehicle suspension dynamics for control of damping," *Symmetry*, Vol. 13, No. 7, p. 1149, Jun. 2021, https://doi.org/10.3390/sym13071149

[74] A. Čerškus, V. Ušinskis, N. Šešok, I. Iljin, and V. Bučinskas, "Optimization of damping in a semi-active car suspension system with various locations of masses," *Applied Sciences*, Vol. 13, No. 9, p. 5371, Apr. 2023, https://doi.org/10.3390/app13095371

[75] Z. Yonglin and Z. Jiafan, "Numerical simulation of stochastic road process using white noise filtration," *Mechanical Systems and Signal Processing*, Vol. 20, No. 2, pp. 363–372, Feb. 2006, https://doi.org/10.1016/j.ymssp.2005.01.009

[76] M. Shinozuka and C.-M. Jan, "Digital simulation of random processes and its applications," *Journal of Sound and Vibration*, Vol. 25, No. 1, pp. 111–128, Nov. 1972, https://doi.org/10.1016/0022-460x(72)90600-1

[77] M. Agostinacchio, D. Ciampa, and S. Olita, "The vibrations induced by surface irregularities in road pavements – a Matlab® approach," *European Transport Research Review*, Vol. 6, No. 3, pp. 267–275, Dec. 2013, https://doi.org/10.1007/s12544-013-0127-8

[78] C. S. Dharankar, M. K. Hada, and S. Chandel, "Numerical generation of road profile through spectral description for simulation of vehicle suspension," *Journal of the Brazilian Society of Mechanical Sciences and Engineering*, Vol. 39, No. 6, pp. 1957–1967, Aug. 2016, https://doi.org/10.1007/s40430-016-0615-6

[79] "Mechanical vibration. Road surface profiles. Reporting of measured data," BSI British Standards, London, ISO 8608:2016(en), Mar. 2022.

[80] P. Andren, "Power spectral density approximations of longitudinal road profiles," *International Journal of Vehicle Design*, Vol. 40, No. 1/2/3, pp. 2–14, Jan. 2006, https://doi.org/10.1504/ijvd.2006.008450

[81] T. Lenkutis, A. Čerškus, N. Šešok, A. Dzedzickis, and V. Bučinskas, "Road surface profile synthesis: assessment of suitability for simulation," *Symmetry*, Vol. 13, No. 1, p. 68, Dec. 2020, https://doi.org/10.3390/sym13010068

[82] V. Bucinskas, P. Mitrouchev, E. Sutinys, N. Sesok, I. Iljin, and I. Morkvenaite-Vilkonciene, "Evaluation of comfort level and harvested energy in the vehicle using controlled damping," *Energies*, Vol. 10, No. 11, p. 1742, Oct. 2017, https://doi.org/10.3390/en10111742

[83] J. Wu, H. Zhou, Z. Liu, and M. Gu, "Ride comfort optimization via speed planning and preview semi-active suspension control for autonomous vehicles on uneven roads," *IEEE Transactions on Vehicular Technology*, Vol. 69, No. 8, pp. 8343–8355, Aug. 2020, https://doi.org/10.1109/tvt.2020.2996681

[84] H. Basargan, A. Mihály, P. Gáspár, and O. Sename, "Cloud-based adaptive semi-active suspension control for improving driving comfort and road holding," *IFAC-PapersOnLine*, Vol. 55, No. 14, pp. 89–94, Jan. 2022, https://doi.org/10.1016/j.ifacol.2022.07.588

Appendix

Table A1. Dependence of the damping on vehicle speed and road waviness (Cases: one coefficient (1P), optimization for driver and front passenger $\left(\begin{smallmatrix}1 & 1\\ 0 & 0\end{smallmatrix}\right)$)

	Damping coefficients, Ns/m				
Waviness	20 km/h	50 km/h	70 km/h	90 km/h	130 km/h
$w_1 = 1; w_2 = 0.5$	1133	1176	1220	1131	1271
$w_1 = 2; w_2 = 0.5$	1130	1213	1517	1443	1621
$w_1 = 4; w_2 = 0.5$	1124	1411	2584	2902	2640
$w_1 = 6; w_2 = 0.5$	1114	1967	4914	6122	4033
$w_1 = 1; w_2 = 1$	1333	1385	1369	1198	1299
$w_1 = 2; w_2 = 1$	1328	1441	1707	1550	1652
$w_1 = 4; w_2 = 1$	1317	1717	2887	3099	2665
$w_1 = 6; w_2 = 1$	1301	2421	5444	6330	4050
$w_1 = 1; w_2 = 2$	1884	1902	1679	1326	1335
$w_1 = 2; w_2 = 2$	1867	2003	2094	1741	1691
$w_1 = 4; w_2 = 2$	1836	2437	3479	3416	2688
$w_1 = 6; w_2 = 2$	1795	3447	6472	6657	4068
$w_1 = 1; w_2 = 3$	2817	2501	1960	1438	1355
$w_1 = 2; w_2 = 3$	2768	2652	2436	1892	1713
$w_1 = 4; w_2 = 3$	2672	3265	4025	3644	2705
$w_1 = 6; w_2 = 3$	2570	4703	7454	6872	4076

Table A2. Dependence of the damping on vehicle speed and road waviness (Cases: one coefficient (1P), optimization for driver and rear left passenger $\left(\begin{smallmatrix}1 & 0\\ 1 & 0\end{smallmatrix}\right)$)

	Damping coefficients, Ns/m				
Waviness	20 km/h	50 km/h	70 km/h	90 km/h	130 km/h
$w_1 = 1; w_2 = 0.5$	1407	1400	1801	1386	1525
$w_1 = 2; w_2 = 0.5$	1399	1516	2311	1940	1809
$w_1 = 4; w_2 = 0.5$	1381	2012	4156	4563	2680
$w_1 = 6; w_2 = 0.5$	1353	3121	8478	9344	3744
$w_1 = 1; w_2 = 1$	1698	1644	2010	1462	1547
$w_1 = 2; w_2 = 1$	1685	1804	2574	2078	1830
$w_1 = 4; w_2 = 1$	1654	2451	4596	4770	2702
$w_1 = 6; w_2 = 1$	1615	3823	9204	9485	3753
$w_1 = 1; w_2 = 2$	2517	2270	2401	1602	1568
$w_1 = 2; w_2 = 2$	2476	2529	3061	2301	1862
$w_1 = 4; w_2 = 2$	2412	3459	5400	5075	2725
$w_1 = 6; w_2 = 2$	2317	5549	10501	9672	3763
$w_1 = 1; w_2 = 3$	3869	2996	2732	1716	1583
$w_1 = 2; w_2 = 3$	3772	3350	3472	2456	1878
$w_1 = 4; w_2 = 3$	3597	4638	6097	5253	2736
$w_1 = 6; w_2 = 3$	3377	7787	11634	9791	3767

Table A3. Dependence of the damping on vehicle speed and road waviness (Cases: one coefficient (1P), optimization for driver and all passengers $\left(\begin{smallmatrix}1 & 1\\ 1 & 1\end{smallmatrix}\right)$)

	Damping coefficients, Ns/m				
Waviness	20 km/h	50 km/h	70 km/h	90 km/h	130 km/h
$w_1 = 1; w_2 = 0.5$	1380	1335	1789	1332	1430
$w_1 = 2; w_2 = 0.5$	1371	1448	2312	1890	1707
$w_1 = 4; w_2 = 0.5$	1352	1945	4241	4612	2609
$w_1 = 6; w_2 = 0.5$	1324	3073	8755	9495	3736
$w_1 = 1; w_2 = 1$	1679	1586	2016	1415	1452
$w_1 = 2; w_2 = 1$	1664	1751	2603	2043	1734
$w_1 = 4; w_2 = 1$	1638	2411	4715	4842	2635
$w_1 = 6; w_2 = 1$	1595	3824	9471	9643	3749
$w_1 = 1; w_2 = 2$	2533	2254	2439	1577	1478
$w_1 = 2; w_2 = 2$	2492	2525	3129	2295	1764
$w_1 = 4; w_2 = 2$	2424	3500	5552	5163	2664
$w_1 = 6; w_2 = 2$	2329	5721	10748	9825	3763
$w_1 = 1; w_2 = 3$	3952	3043	2795	1711	1492
$w_1 = 2; w_2 = 3$	3845	3424	3567	2480	1782
$w_1 = 4; w_2 = 3$	3673	4777	6283	5370	2679
$w_1 = 6; w_2 = 3$	3459	8191	11890	9947	3770

Table A4. Dependence of the damping on vehicle speed and road waviness (Cases: two different coefficients for front and rear (2P) respectively top and bottom values, optimization for driver $\left(\begin{smallmatrix}1 & 0\\ 0 & 0\end{smallmatrix}\right)$)

	Damping coefficients, Ns/m				
Waviness	20 km/h	50 km/h	70 km/h	90 km/h	130 km/h
$w_1 = 1; w_2 = 0.5$	1000 7762	1000 15000	1000 15000	1000 14998	1000 14998
$w_1 = 2; w_2 = 0.5$	1000 7765	1000 15000	1000 15000	1000 14990	1327 12304
$w_1 = 4; w_2 = 0.5$	1000 7732	1000 15000	1000 15000	1378 9035	2328 8714
$w_1 = 6; w_2 = 0.5$	1000 8704	1000 15000	1181 14512	2828 8349	3488 6656
$w_1 = 1; w_2 = 1$	1046 7544	1000 15000	1000 15000	1000 14998	1000 14998
$w_1 = 2; w_2 = 1$	1033 7721	1000 15000	1000 15000	1000 14989	1390 14881
$w_1 = 4; w_2 = 1$	1037 7438	1000 15000	1000 15000	1489 8960	2354 8947
$w_1 = 6; w_2 = 1$	1039 7418	1000 15000	1392 14104	3087 8440	3494 6660
$w_1 = 1; w_2 = 2$	1448 6674	1301 15000	1000 15000	1000 14999	1000 14999
$w_1 = 2; w_2 = 2$	1448 7047	1286 15000	1000 15000	1000 14989	1402 12340
$w_1 = 4; w_2 = 2$	1449 6850	1276 15000	1193 15000	1680 8928	2381 8900
$w_1 = 6; w_2 = 2$	1449 6560	1327 15000	1877 13976	3496 8570	3506 6656
$w_1 = 1; w_2 = 3$	2015 7869	1623 15000	1000 15000	1000 14999	1000 14999
$w_1 = 2; w_2 = 3$	1989 7840	1610 15000	1108 15000	1098 12138	1425 12143
$w_1 = 4; w_2 = 3$	2007 7279	1604 15000	1451 15000	1827 8900	2393 8875
$w_1 = 6; w_2 = 3$	2048 8854	1691 15000	2458 13961	3762 8624	3512 6665

Table A5. Dependence of the damping on vehicle speed and road waviness (Cases: two different coefficients for front and rear (2P) respectively, top and bottom values, optimization for driver and front passenger ($\begin{smallmatrix}1 & 1\\ 0 & 0\end{smallmatrix}$))

	Damping coefficients, Ns/m				
Waviness	20 km/h	50 km/h	70 km/h	90 km/h	130 km/h
$w_1 = 1; w_2 = 0.5$	1000 7930	1000 15000	1000 15000	1000 14994	1000 14990
$w_1 = 2; w_2 = 0.5$	1000 7915	1000 15000	1000 15000	1000 11799	1128 11804
$w_1 = 4; w_2 = 0.5$	1000 7882	1000 15000	1000 15000	1179 9404	2074 8514
$w_1 = 6; w_2 = 0.5$	1000 8500	1000 15000	1015 15000	2378 8524	3251 6682
$w_1 = 1; w_2 = 1$	1000 7653	1000 15000	1000 15000	1000 14995	1000 14991
$w_1 = 2; w_2 = 1$	1000 7589	1000 15000	1000 15000	1000 11912	1157 11908
$w_1 = 4; w_2 = 1$	1000 7560	1000 15000	1000 15000	1282 9312	2104 8521
$w_1 = 6; w_2 = 1$	1000 7469	1000 15000	1190 14996	2697 8582	3266 6687
$w_1 = 1; w_2 = 2$	1386 7217	1262 15000	1000 15000	1000 14995	1000 14991
$w_1 = 2; w_2 = 2$	1387 7119	1248 15000	1000 15000	1000 12126	1199 11785
$w_1 = 4; w_2 = 2$	1387 6936	1241 15000	1080 15000	1482 9182	2145 8527
$w_1 = 6; w_2 = 2$	1389 6676	1290 15000	1666 14249	3234 8713	3284 6692
$w_1 = 1; w_2 = 3$	1996 7994	1612 15000	1000 15000	1000 14995	1000 14990
$w_1 = 2; w_2 = 3$	1980 7693	1603 15000	1000 15000	1000 12225	1222 11769
$w_1 = 4; w_2 = 3$	1973 7335	1603 15000	1325 15000	1649 9122	2168 8542
$w_1 = 6; w_2 = 3$	2001 8519	1689 15000	2286 14140	3620 8808	3294 6695

Table A6. Dependence of the damping on vehicle speed and road waviness (Cases: two different coefficients for front and rear (2P) respectively, top and bottom values, optimization for driver and all passengers ($\begin{smallmatrix}1 & 1\\ 1 & 1\end{smallmatrix}$))

	Damping coefficients, Ns/m				
Waviness	20 km/h	50 km/h	70 km/h	90 km/h	130 km/h
$w_1 = 1; w_2 = 0.5$	1000 2610	1100 2254	1000 3627	1000 2901	1095 2721
$w_1 = 2; w_2 = 0.5$	1000 2572	1080 2880	1000 5240	1021 4950	1399 3054
$w_1 = 4; w_2 = 0.5$	1003 2510	1000 5480	1000 10355	1344 8520	2291 3828
$w_1 = 6; w_2 = 0.5$	1010 2410	1000 12714	1278 15000	3443 11287	3496 4159
$w_1 = 1; w_2 = 1$	1173 3303	1280 2822	1000 4249	1000 3362	1096 2896
$w_1 = 2; w_2 = 1$	1175 3246	1247 3711	1000 6026	1083 5370	1411 3207
$w_1 = 4; w_2 = 1$	1179 3145	1161 7036	1116 10745	1456 8600	2303 3892

ISSN PRINT 1392-8716, ISSN ONLINE 2538-8460

$w_1 = 6; w_2 = 1$	1184 3022	1020 15000	1569 15000	3811 11382	3505 4169
$w_1 = 1; w_2 = 2$	1552 5010	1734 4126	1151 5151	1043 4059	1096 3108
$w_1 = 2; w_2 = 2$	1554 4907	1671 5392	1226 6892	1172 5879	1424 3393
$w_1 = 4; w_2 = 2$	1558 4716	1522 9540	1420 11134	1682 8689	2327 3957
$w_1 = 6; w_2 = 2$	1560 4499	1417 15000	2393 15000	4370 11513	3521 4182
$w_1 = 1; w_2 = 3$	2166 7032	2279 5184	1346 5679	1109 4462	1096 3226
$w_1 = 2; w_2 = 3$	2157 6901	2180 6624	1453 7370	1257 6146	1432 3488
$w_1 = 4; w_2 = 3$	2152 6508	1971 10995	1763 11326	1864 8737	2338 3991
$w_1 = 6; w_2 = 3$	2149 6167	1902 15000	3334 15000	4725 11565	3525 4191

Table A7. Dependence of the damping on vehicle speed and road waviness
(Cases: four different coefficients (4P), optimization for driver $\left(\begin{smallmatrix}1 & 0\\ 0 & 0\end{smallmatrix}\right)$)

	Damping coefficients, Ns/m									
Waviness	20 km/h		50 km/h		70 km/h		90 km/h		130 km/h	
$w_1 = 1; w_2 = 0.5$	1000	1000	1000	1000	1000	1000	1000	1000	1000	1000
	5920	9043	15000	15000	14995	15000	14990	15000	14981	15000
$w_1 = 2; w_2 = 0.5$	1000	1000	1000	1000	1000	1000	1000	1000	1000	1393
	5832	8980	15000	15000	14992	15000	14979	15000	6561	15000
$w_1 = 4; w_2 = 0.5$	1000	1000	1000	1000	1000	1000	1372	1049	1000	2380
	5752	8923	15000	15000	14990	15000	8051	10219	1000	8777
$w_1 = 6; w_2 = 0.5$	1000	1000	1000	1000	1000	2789	1697	15000	1000	4573
	5722	8846	15000	15000	15000	11099	12283	5452	1000	6777
$w_1 = 1; w_2 = 1$	1000	1000	1000	1000	1000	1000	1000	1000	1000	1000
	5572	8781	15000	15000	14997	15000	14994	15000	14985	15000
$w_1 = 2; w_2 = 1$	1000	1000	1000	1000	1000	1000	1000	1000	1000	1405
	5524	8714	15000	15000	14995	15000	14982	15000	6604	15000
$w_1 = 4; w_2 = 1$	1000	1000	1000	1000	1000	1000	1607	1000	1000	2381
	5402	8617	15000	15000	14991	15000	8406	9806	1000	8771
$w_1 = 6; w_2 = 1$	1000	1000	1000	1044	1000	5239	2020	14706	1000	4583
	5337	8501	15000	15000	15000	9236	12602	5129	1000	6775
$w_1 = 1; w_2 = 2$	1544	1000	1499	1000	1000	1000	1000	1000	1000	1000
	5964	8015	15000	15000	15000	15000	14999	15000	10976	15000
$w_1 = 2; w_2 = 2$	1571	1000	1461	1000	1000	1000	1001	1000	1000	1417
	6275	7743	15000	15000	14998	15000	14986	15000	6417	14997
$w_1 = 4; w_2 = 2$	1562	1000	1383	1095	1278	1000	1949	1037	1000	2382
	5987	7620	15000	15000	13388	15000	8872	9144	1000	8783
$w_1 = 6; w_2 = 2$	1588	1000	1392	1223	1000	9881	2574	13786	1000	4583
	5474	6784	15000	15000	15000	7718	13227	4617	1000	6778
$w_1 = 1; w_2 = 3$	2203	1852	1875	1613	1099	1000	1000	1000	1000	1000
	8627	6846	15000	9893	14856	15000	14861	14998	11083	15000
$w_1 = 2; w_2 = 3$	2049	2042	1875	1421	1258	1000	1126	1000	1000	1451
	9941	6678	15000	11609	15000	15000	11260	12905	5948	13804
$w_1 = 4; w_2 = 3$	2169	1947	1859	1275	1703	1000	2143	1329	1000	2381
	10867	7772	15000	14057	14839	15000	9490	8520	1000	8781
$w_1 = 6; w_2 = 3$	1989	2315	1962	1284	1277	12990	2940	13473	1000	4586
	7725	5906	15000	15000	15000	6847	13696	4315	1000	6777

Table A8. Dependence of the damping on vehicle speed and road waviness
(Cases: four different coefficients (4P), optimization for driver and front passenger $\left(\begin{smallmatrix}1 & 1\\ 0 & 0\end{smallmatrix}\right)$)

	Damping coefficients, Ns/m									
Waviness	20 km/h		50 km/h		70 km/h		90 km/h		130 km/h	
$w_1 = 1; w_2 = 0.5$	1000	1000	1000	1000	1000	1000	1000	1000	1000	1000
	7402	9033	15000	15000	14999	15000	14994	15000	14980	15000
$w_1 = 2; w_2 = 0.5$	1000	1000	1000	1000	1000	1000	1000	1000	1252	1000
	7375	8993	15000	15000	14999	15000	14985	14997	10826	13208
$w_1 = 4; w_2 = 0.5$	1000	1000	1000	1000	1000	1000	1390	1000	1000	3159
	7349	8881	14950	15000	14949	15000	9356	9538	5259	10889
$w_1 = 6; w_2 = 0.5$	1000	1000	1000	1000	1105	1000	4528	1000	1922	4548
	7288	8800	15000	15000	14998	15000	8290	9684	4478	8243
$w_1 = 1; w_2 = 1$	1000	1000	1000	1000	1000	1000	1000	1000	1000	1000
	7148	8550	15000	15000	15000	15000	14994	15000	14980	15000
$w_1 = 2; w_2 = 1$	1000	1000	1000	1000	1000	1000	1000	1000	1308	1000
	7069	8549	15000	15000	15000	15000	11546	12628	10920	13081
$w_1 = 4; w_2 = 1$	1000	1000	1000	1000	1000	1000	1559	1000	1000	3188
	7053	8403	15000	15000	15000	15000	9367	9456	5258	10889
$w_1 = 6; w_2 = 1$	1000	1000	1000	1000	1397	1000	4778	1198	1993	4512
	6967	8291	15000	15000	14442	15000	8234	9836	4565	8232
$w_1 = 1; w_2 = 2$	1329	1442	1145	1381	1000	1000	1000	1000	1000	1000
	6534	7463	15000	15000	15000	15000	14993	15000	14978	15000
$w_1 = 2; w_2 = 2$	1327	1461	1139	1359	1000	1000	1000	1000	1372	1000
	6632	7714	15000	15000	15000	15000	11614	12920	11118	13035
$w_1 = 4; w_2 = 2$	1330	1443	1139	1342	1035	1114	1644	1307	1029	3212
	6504	7517	15000	15000	15000	15000	9120	9361	5341	10902
$w_1 = 6; w_2 = 2$	1331	1450	1218	1365	2048	1319	4965	1762	2067	4484
	6261	7241	15000	15000	13741	14979	8173	9855	4653	8209
$w_1 = 1; w_2 = 3$	1861	2102	1403	1829	1000	1000	1000	1000	1000	1000
	7298	7727	15000	15000	15000	15000	14991	15000	12103	15000
$w_1 = 2; w_2 = 3$	1941	2004	1396	1810	1000	1048	1000	1000	1398	1012
	7027	8421	15000	15000	15000	15000	11654	12937	11354	13070
$w_1 = 4; w_2 = 3$	1847	2165	1410	1803	1266	1386	1742	1539	1192	3101
	6716	7906	15000	15000	15000	15000	8983	9320	5667	10791
$w_1 = 6; w_2 = 3$	1867	2079	1541	1841	2993	1676	5001	2301	2108	4459
	6540	7219	15000	15000	13255	15000	8220	9790	4697	8189

Table A9. Dependence of the damping on vehicle speed and road waviness
(Cases: four different coefficients (4P), optimization for driver and rear left passenger $\left(\begin{smallmatrix}1 & 0\\ 1 & 0\end{smallmatrix}\right)$)

	Damping coefficients, Ns/m									
Waviness	20 km/h		50 km/h		70 km/h		90 km/h		130 km/h	
$w_1 = 1; w_2 = 0.5$	1000	1440	1081	1204	1000	1000	1000	1000	1000	1613
	1865	3680	1805	4548	2140	6597	2195	5003	1825	5059
$w_1 = 2; w_2 = 0.5$	1000	1451	1020	1209	1000	1000	1000	1241	1000	2042
	1835	3612	2023	5721	3285	8194	3603	6431	1849	5399
$w_1 = 4; w_2 = 0.5$	1000	1459	1000	1185	1000	2622	1369	2125	1567	3537
	1789	3503	3387	8658	9720	10350	8781	7462	1985	4510
$w_1 = 6; w_2 = 0.5$	1000	1478	1000	1076	1000	6314	2173	8717	3169	5336
	1713	3342	9987	15000	15000	10692	15000	6648	3375	3610
$w_1 = 1; w_2 = 1$	1000	1699	1184	1550	1000	1498	1000	1104	1000	1533
	2513	4130	2136	4613	2705	6284	2573	5190	1900	5117
$w_1 = 2; w_2 = 1$	1000	1712	1143	1529	1000	1751	1000	1365	1000	2001
	2446	4060	2620	5786	4326	7792	4197	6587	1906	5482
$w_1 = 4; w_2 = 1$	1000	1736	1003	1478	1000	3664	1516	2390	1701	3406
	2383	3907	5339	9422	11530	9846	9215	7222	2163	4427
$w_1 = 6; w_2 = 1$	1000	1759	1000	1362	1000	7334	2419	8832	3278	5174
	2279	3732	13006	15000	15000	10297	15000	6559	3531	3576

ISSN PRINT 1392-8716, ISSN ONLINE 2538-8460

$w_1 = 1; w_2 = 2$	1369 2168 4710 4836	1363 2797 3867 4575	1000 2390 4274 5898	1000 1267 3213 5260	1000 1404 2035 5290
$w_1 = 2; w_2 = 2$	1363 2176 4565 4775	1290 2722 5131 5739	1000 2892 6395 7023	1000 1542 4984 6723	1000 1921 2002 5609
$w_1 = 4; w_2 = 2$	1367 2165 4457 4626	1102 2601 9722 9013	1000 5550 14280 8744	1832 2731 9828 6837	1910 3159 2477 4325
$w_1 = 6; w_2 = 2$	1370 2285 4173 4106	1000 2377 15000 14460	1000 9551 15000 9790	2819 8911 15000 6425	3363 5011 3672 3565
$w_1 = 1; w_2 = 3$	1945 3053 8392 5586	1413 5202 7451 4033	1000 3100 5425 5600	1000 1343 3709 5407	1000 1310 2142 5409
$w_1 = 2; w_2 = 3$	1973 2991 8029 5317	1296 5141 8894 5030	1000 3959 7938 6630	1118 1572 5482 6616	1000 1870 2066 5692
$w_1 = 4; w_2 = 3$	1978 2923 7841 5113	1013 4831 14898 7529	1000 6855 15000 8321	2076 3025 10310 6542	2050 2986 2709 4271
$w_1 = 6; w_2 = 3$	1947 2918 7296 4564	1123 4008 15000 11802	1158 11724 15000 9393	3117 8997 15000 6350	3399 4959 3720 3549

Table A10. The maximum difference in the RMS value of vertical acceleration (for all four positions and the sum) relative to the reference of the corresponding RMS values of vertical acceleration for the corresponding speed and road profile when optimized for the driver with the same number of damping values. FL – front left (driver), FR – front right passenger, RL – rear left passenger, RR – rear right passenger

Damping values	Optimized for		Difference, m s^{-2}				
			RMS(a_{FL})	RMS(a_{FR})	RMS(a_{RR})	RMS(a_{RL})	ΣRMS
1P	$\begin{pmatrix}1&0\\0&0\end{pmatrix}$		as reference				
	$\begin{pmatrix}1&1\\0&0\end{pmatrix}$	min	0.0000	–0.0069	–0.0207	–0.0200	–0.0411
		max	0.0023	0.0000	0.0331	0.0313	0.0089
	$\begin{pmatrix}1&0\\1&0\end{pmatrix}$	min	0.0002	–0.0034	–0.5118	–0.4867	–0.6403
		max	0.1828	0.1754	–0.0004	–0.0003	0.0025
	$\begin{pmatrix}1&1\\1&1\end{pmatrix}$	min	4E–5	–0.0052	–0.5335	–0.5069	–0.6421
		max	0.2040	0.1943	0.0010	0.0008	–5E-5
2P	$\begin{pmatrix}1&0\\0&0\end{pmatrix}$		as reference				
	$\begin{pmatrix}1&1\\0&0\end{pmatrix}$	min	–0.0046	–0.0222	–0.0929	–0.0922	–0.2082
		max	0.0056	0.0000	0.0078	0.0118	0.0141
	$\begin{pmatrix}1&0\\1&0\end{pmatrix}$	min	–0.0005	–0.0001	–0.3619	–0.3865	–0.5774
		max	0.1317	0.1607	–0.0014	–0.0021	0.0046
	$\begin{pmatrix}1&1\\1&1\end{pmatrix}$	min	–0.0007	–0.0010	–0.3566	–0.3793	–0.5841
		max	0.0980	0.1163	0.0002	–0.0005	–0.0003
4P	$\begin{pmatrix}1&0\\0&0\end{pmatrix}$		as reference				
	$\begin{pmatrix}1&1\\0&0\end{pmatrix}$	min	–0.0071	–0.4920	–0.5592	–0.3213	–0.7696
		max	0.2110	0.0003	0.4130	0.1059	0.1292
	$\begin{pmatrix}1&0\\1&0\end{pmatrix}$	min	–2E–5	–0.3487	–0.2843	–1.0499	–0.5489
		max	0.5575	0.2304	0.4905	–0.0028	0.1934
	$\begin{pmatrix}1&1\\1&1\end{pmatrix}$	min	–2E–5	–0.4465	–0.5684	–0.4432	–0.8967
		max	0.1788	0.0709	0.1454	0.0693	–3E-5

Table A11. The maximum percentage change in the RMS value of vertical acceleration (for the four positions and the sum) relative to the reference of the corresponding RMS values of vertical acceleration for the corresponding speed and road profile when optimized for the entire crew $\left(\begin{smallmatrix}1&1\\1&1\end{smallmatrix}\right)$ with four damping values (4P). FL – front left (driver), FR – front right passenger, RL – rear left passenger, RR – rear right passenger

Dampin g values	Optimized for		Percentage change, %				
			RMS(a_{FL})	RMS(a_{FR})	RMS(a_{RR})	RMS(a_{RL})	ΣRMS
1P	$\begin{pmatrix}1&0\\0&0\end{pmatrix}$	min	2.34	–7.15	–5.02	–20.2	0.08
		max	38.8	38.5	33.4	27.1	33.1
		min	2.41	–7.20	–4.64	–20.34	–0.01

	$\binom{1\ 1}{0\ 0}$	max	38.8	38.5	36.3	27.9	34.0
	$\binom{1\ 0}{1\ 0}$	min	2.71	–7.08	–5.50	–20.31	–0.19
		max	49.4	48.5	16.1	11.1	25.8
	$\binom{1\ 1}{1\ 1}$	min	2.48	–7.08	–5.09	–20.36	–0.19
		max	50.6	49.7	16.1	11.1	25.8
2P	$\binom{1\ 0}{0\ 0}$	min	–9.48	–15.5	–0.03	–5.12	0.01
		max	12.4	1.20	46.7	49.4	18.1
	$\binom{1\ 1}{0\ 0}$	min	–9.48	–16.37	–0.03	–4.84	0.01
		max	12.6	0.41	46.4	49.4	16.2
	$\binom{1\ 0}{1\ 0}$	min	0.14	–7.68	–5.08	–18.0	–0.39
		max	21.3	4.55	12.1	0.78	0.46
	$\binom{1\ 1}{1\ 1}$	min	–0.01	–9.55	–4.61	–16.7	–0.45
		max	19.8	3.68	13.4	0.97	0.25
4P	$\binom{1\ 0}{0\ 0}$	min	–9.53	–9.71	–4.69	–3.51	0.00
		max	0.00	22.6	46.4	48.8	15.9
	$\binom{1\ 1}{0\ 0}$	min	–9.48	–12.7	–0.11	–0.02	0.01
		max	3.81	–0.06	46.4	48.8	16.1
	$\binom{1\ 0}{1\ 0}$	min	–6.99	–3.93	–1.82	–16.0	–0.29
		max	20.1	30.8	11.6	–0.02	6.32
	$\binom{1\ 1}{1\ 1}$	as reference					

Table A12. The maximum difference in the RMS value of vertical acceleration (for the four positions and the sum) relative to the reference of the corresponding RMS values of vertical acceleration for the corresponding speed and road profile when optimized for the entire crew ($\binom{11}{11}$) with four damping values (4P). FL – front left (driver), FR – front right passenger, RL – rear left passenger, RR – rear right passenger

Damping values			difference, m s^{-2}				
	Optimized for		RMS(a_{FL})	RMS(a_{FR})	RMS(a_{RR})	RMS(a_{RL})	ΣRMS
1P	$\binom{1\ 0}{0\ 0}$	min	0.0127	–0.1700	–0.0382	–0.5419	0.0092
		max	0.4999	0.5686	0.6210	0.5543	2.2440
	$\binom{1\ 1}{0\ 0}$	min	0.0127	–0.1710	–0.0353	–0.5489	–0.0007
		max	0.5001	0.5680	0.6406	0.5732	2.2820
	$\binom{1\ 0}{1\ 0}$	min	0.0180	–0.1683	–0.0434	–0.5678	–0.0213
		max	0.6827	0.7439	0.3083	0.1282	1.6036
	$\binom{1\ 1}{1\ 1}$	min	0.0190	–0.1684	–0.0522	–0.5683	–0.0213
		max	0.7039	0.7628	0.3084	0.1281	1.6019
2P	$\binom{1\ 0}{0\ 0}$	min	–0.0629	–0.3433	–0.0003	–0.1952	0.0003
		max	0.2673	0.0235	0.5970	0.3527	0.5910
	$\binom{1\ 1}{0\ 0}$	min	–0.0629	–0.3540	–0.0003	–0.1845	0.0003
		max	0.2715	0.0081	0.6039	0.3527	0.5405
	$\binom{1\ 0}{1\ 0}$	min	0.0003	–0.1826	–0.0836	–0.5579	–0.0388
		max	0.3990	0.0897	0.3157	0.0228	0.0272
	$\binom{1\ 1}{1\ 1}$	min	–0.0002	–0.2270	–0.0822	–0.5180	–0.0444
		max	0.3653	0.0725	0.3429	0.0244	0.0186
4P	$\binom{1\ 0}{0\ 0}$	min	–0.1787	–0.0708	–0.1453	–0.0693	3E-05
		max	2E–05	0.4464	0.5684	0.4432	0.8966
	$\binom{1\ 1}{0\ 0}$	min	–0.0629	–0.2185	–0.0033	–0.0001	0.0003
		max	0.0810	–0.0006	0.3103	0.3527	0.5405
	$\binom{1\ 0}{1\ 0}$	min	–0.1420	–0.0933	–0.0112	–0.6067	–0.0151
		max	0.4274	0.3095	0.3451	–1E-04	0.3619
	$\binom{1\ 1}{1\ 1}$	as reference					

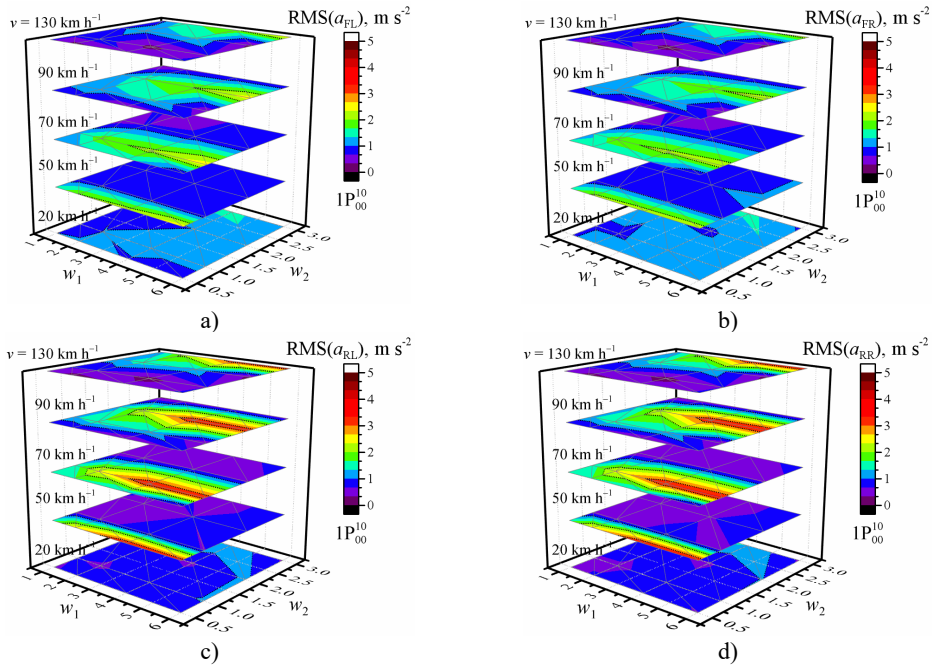

Fig. A1. Dependence of the RMS value of vertical acceleration a) of the driver (front left); b) of the front right passenger; c) of the rear left passenger; and d) of the rear right passenger; on road profile waviness w_1 and w_2 when vehicle speed is 20 km/h, 50 km/h, 70 km/h, 90 km/h or 130 km/h and optimized for the driver with one damping value. The black dotted line shows values of major ticks

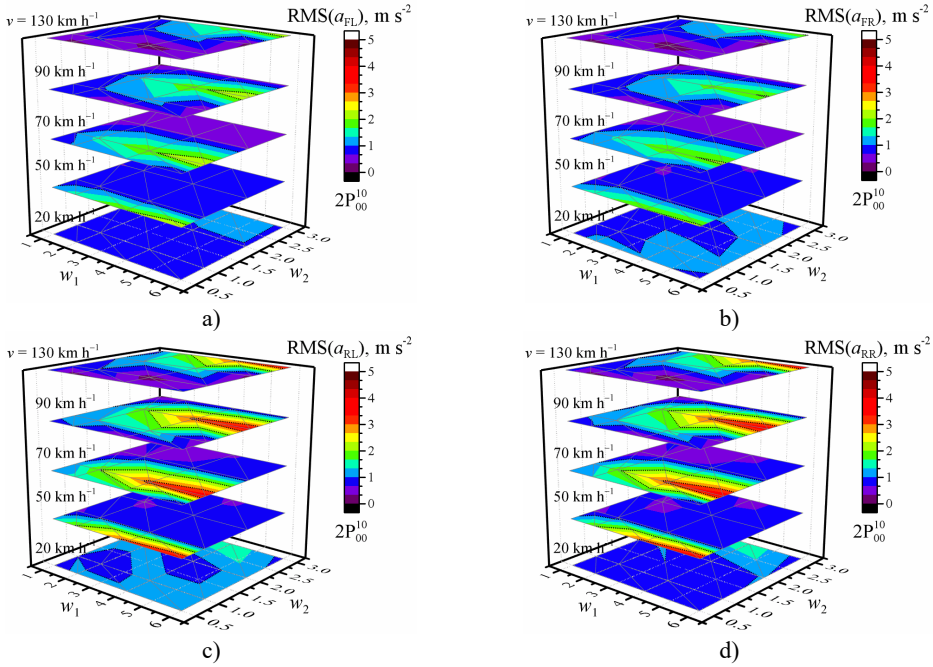

Fig. A2. Dependence of the RMS value of vertical acceleration a) of the driver (front left); b) of the front right passenger; c) of the rear left passenger; and d) of the rear right passenger; on road profile waviness w_1 and w_2 when vehicle speed is 20 km/h, 50 km/h, 70 km/h, 90 km/h or 130 km/h and optimized for the driver with two damping values. The black dotted line shows values of major ticks

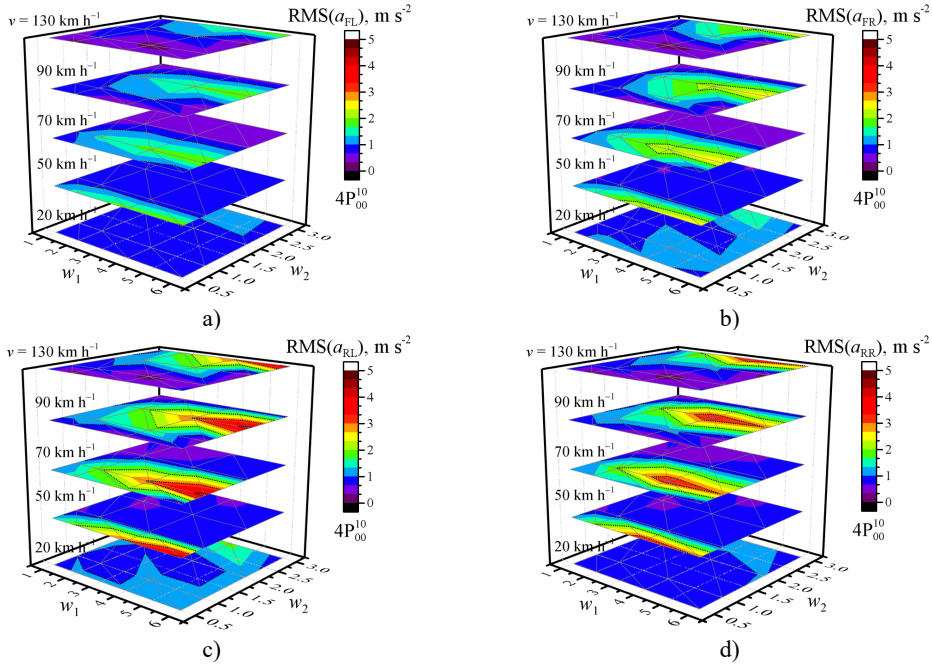

Fig. A3. Dependence of the RMS value of vertical acceleration a) of the driver (front left); b) of the front right passenger; c) of the rear left passenger; and d) of the rear right passenger; on road profile waviness w_1 and w_2 when vehicle speed is 20 km/h, 50 km/h, 70 km/h, 90 km/h or 130 km/h and optimized for the driver with four damping values. The black dotted line shows values of major ticks.

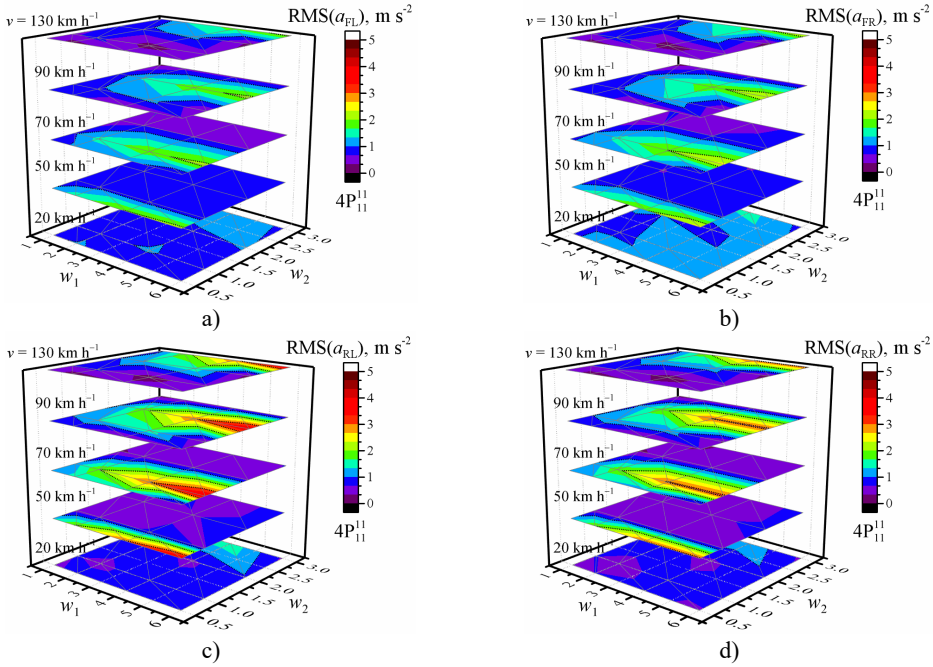

Fig. A4. Dependence of the RMS value of vertical acceleration a) of the driver (front left); b) of the front right passenger; c) of the rear left passenger; and d) of the rear right passenger; on road profile waviness w_1 and w_2 when vehicle speed is 20 km/h, 50 km/h, 70 km/h, 90 km/h or 130 km/h and optimized for the entire crew with four damping values. The black dotted line shows values of major ticks

ISSN PRINT 1392-8716, ISSN ONLINE 2538-8460

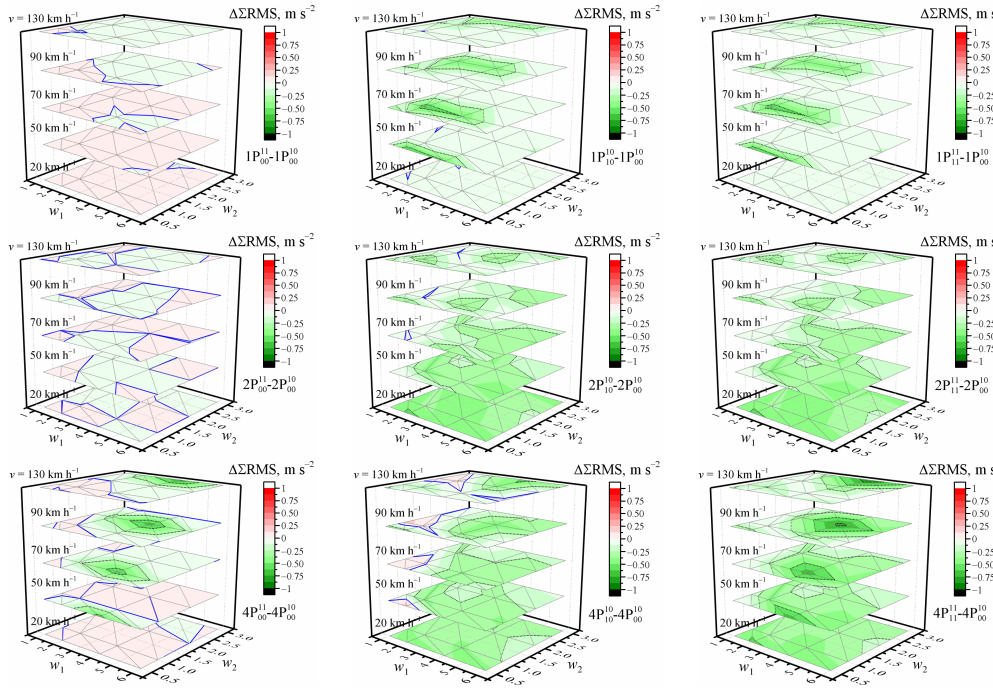

Fig. A5. Dependence of the difference in the sum of the RMS values of vertical accelerations of the entire crew on road profile waviness w_1 and w_2 when vehicle speed is 20 km/h, 50 km/h, 70 km/h, 90 km/h or 130 km/h when optimized for various cases with a), b), c) – one damping value; d), e), f) – two damping values; g), h), i) – four damping values as parameter relative to the reference of the corresponding sum of the RMS values of vertical acceleration for the corresponding speed and road profile when optimized for the driver with the same number of damping values. The black dotted line shows the values of major ticks. The solid blue line is zero

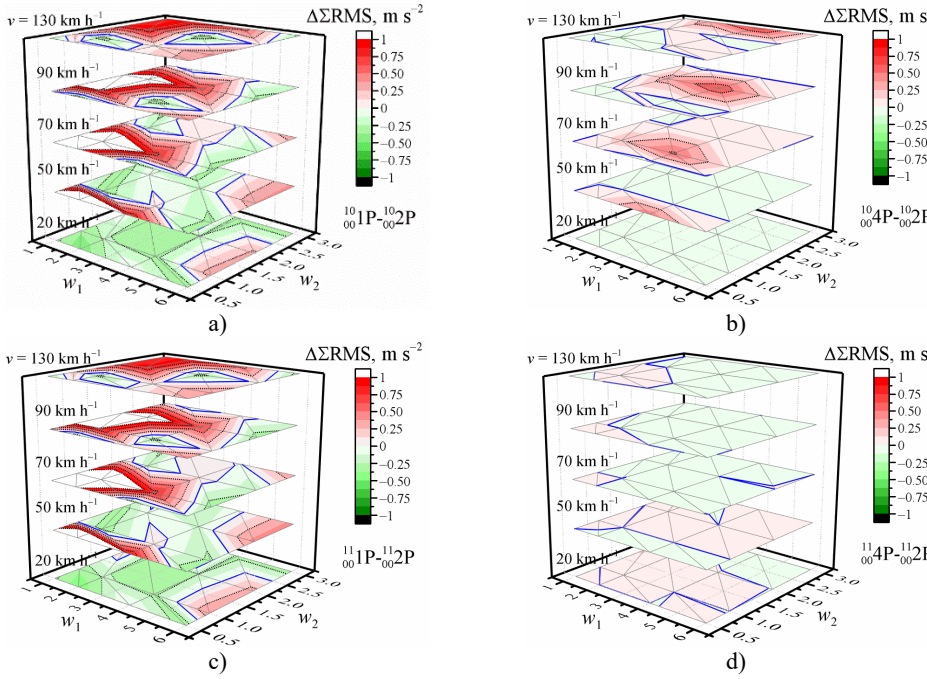

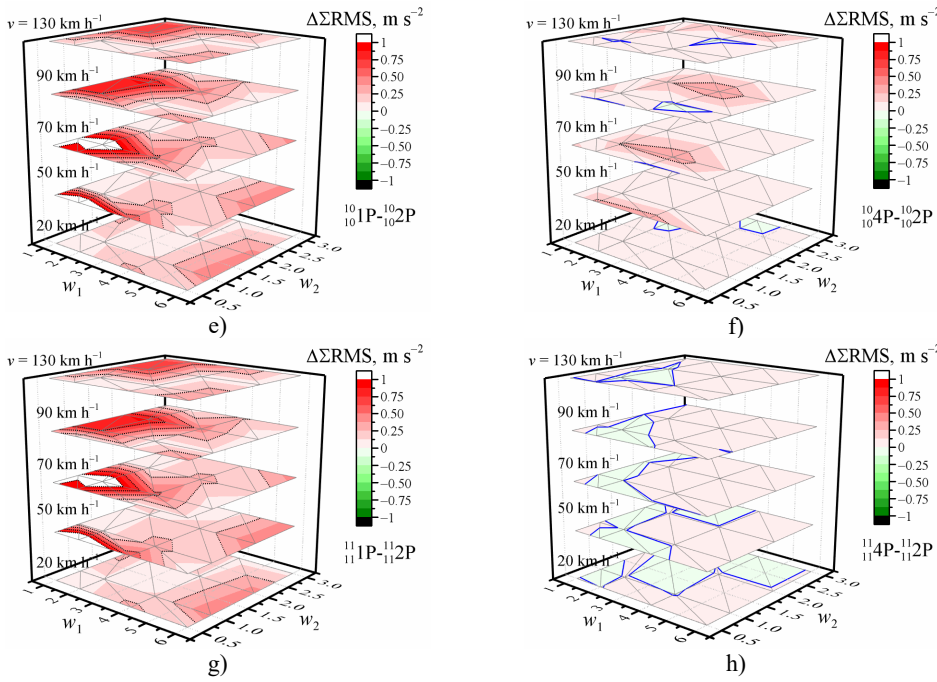

Fig. A6. Dependence of the difference in the sum of the RMS values of vertical accelerations of the entire crew on road profile waviness w_1 and w_2 when vehicle speed is 20 km/h, 50 km/h, 70 km/h, 90 km/h, or 130 km/h when optimized a), b) – for the driver;(c), d) – for the driver and front right passenger; e), f) – for the driver and rear left passenger; g), h) – for the entire crew relative to the reference of the corresponding sum of the RMS values of vertical acceleration for the corresponding speed and road profile when optimized for the same case with two damping values. The black dotted line shows the values of major ticks. The solid blue line is zero

Aurimas Čerškus received Ph.D. degree in Semiconductor Physics from Semiconductor Physics Institute and Vilnius University, Vilnius, Lithuania, in 2009. Now he works at Vilnius Gediminas Technical University and State research institute Center for Physical Sciences and Technology. His current research interests include dynamics.

Nikolaj Šešok received Ph.D. degree in field of Dynamics from Vilnius Technical University, Vilnius, Lithuania, in 2000. Now he works at Vilnius Gediminas Technical University as an Associate Professor. His current research interests include dynamical properties of mechanical and mechatronic systems.

Vytautas Bučinskas received Ph.D. degree in the field of Theory of Machines and became an Associate Professor in the Department of Machine Engineering, Vilnius Technical University, Vilnius, Lithuania, in 2002. He got the Professor Position in the same Department in 2012. In 2013, the Department of Mechatronics and Robotics was established, and he took steering chair in it. After merging two Departments, he heads Department of Mechatronics, Robotics and Digital manufacturing. His current research interests include design of mechatronic systems, dynamical properties of mechatronic systems, energy harvesting from vibrations.

ISSN PRINT 1392-8716, ISSN ONLINE 2538-8460